

**Manuscript title:** Pharmacokinetic assessment of cooperative efflux of the multi-targeted kinase inhibitor ponatinib across the blood-brain barrier

**Authors:** Janice K. Laramy, Minjee Kim, Karen E. Parrish, Jann N. Sarkaria, and William F. Elmquist

Brain Barriers Research Center, Department of Pharmaceutics, College of Pharmacy, University of Minnesota, Minneapolis, Minnesota (J.K.L, M.K, K.E.P, W.F.E)

Department of Radiation Oncology, Mayo Clinic, Rochester, Minnesota (J.N.S.)

**Running title:** Cooperative BBB efflux of ponatinib

**Corresponding author**

William F. Elmquist

Professor

Department of Pharmaceutics

University of Minnesota

308 Harvard ST SE

Minneapolis MN 55455

Phone: 612-625-0097; Fax: 612-626-2125

E-mail: [elmqu011@umn.edu](mailto:elmqu011@umn.edu)

**Number of pages**

Number of text pages: 20

Number of tables: 7

Number of figures: 7

Number of references: 35

Number of words in abstract: 247

Number of words in introduction: 654 (excluding text citations)

Number of words in discussion: 1329 (excluding text citations)

**Abbreviations**

AUC, area under the curve

BBB, blood-brain-barrier

*Bcrp*, gene encoding the murine breast cancer resistance protein

CNS, central nervous system

DA, distribution advantage

EGFR, epidermal growth factor receptor

GBM, glioblastoma

K<sub>p</sub>, total brain-to-plasma ratio

K<sub>p,uu</sub>, unbound (free) brain-to-plasma ratio

LC-MS/MS, liquid chromatography–tandem mass spectrometry

*Mdr1*, gene encoding the murine p-glycoprotein

MTT, mean transit time

NCA, non-compartmental analysis

PDGFR- $\alpha$ , platelet-derived growth factor receptor- $\alpha$

PDX, patient-derived xenograft

P-gp, p-glycoprotein

RET, REarranged during Transfection

**Recommended section assignment:** Metabolism, Transport, and Pharmacogenomics

## ABSTRACT

A compartmental blood-brain barrier (BBB) model describing drug transport across the BBB was implemented to evaluate the influence of efflux transporters on the rate and extent of the multi-kinase inhibitor ponatinib penetration across the BBB. In vivo pharmacokinetic studies in wild-type and transporter knockout mice showed that two major BBB efflux transporters, P-glycoprotein (P-gp) and breast cancer resistance protein (Bcrp), cooperate to modulate the brain exposure of ponatinib. The total and free brain-to-plasma ratios ( $K_p$  or  $K_{p,uu}$ ) were approximately 15-fold higher in the triple knockout mice lacking both P-gp and Bcrp (*Mdr1a/b*( $-/-$ )*Bcrp1*( $-/-$ )) compared to the wild-type mice. The triple knockout mice had a greater than an additive increase in the brain exposure of ponatinib when compared to single knockout mice (*Bcrp1*( $-/-$ ) or *Mdr1a/b*( $-/-$ )), suggesting functional compensation of transporter-mediated drug efflux. Based on the BBB model characterizing the observed brain and plasma concentration-time profiles, the brain exit rate constant and clearance out of the brain were approximately 15-fold higher in the wild-type compared to *Mdr1a/b*( $-/-$ )*Bcrp1*( $-/-$ ) mice, resulting in a significant increase in the mean transit time (MTT; the average time spent by ponatinib in the brain in a single passage) in the absence of efflux transporters (P-gp and Bcrp). This study characterized transporter-mediated drug efflux from the brain; a process that reduces the duration and extent of ponatinib exposure in the brain, and has critical implications on the use of targeted drug delivery for brain tumors.

## INTRODUCTION

Nearly 12,000 new cases of glioblastoma (GBM), the most common malignant primary brain cancer, are projected for 2017 (Ostrom et al., 2016). Currently, the 2-year survival rate of GBM patient is only approximately 17%, despite aggressive treatment that combines surgery, radiation, and adjuvant chemotherapy (Ostrom et al., 2016). Many potent anticancer agents, targeting known drivers of GBM, have failed to demonstrate efficacy in clinical trials in the past decade (De Witt Hamer, 2010). Our proteomic analysis of patient-derived xenograft (PDX) GBM tumors has identified overexpression of PDGFR- $\alpha$  and RET, as a possible mechanism of drug resistance (erlotinib and temozolomide) upon orthotopic implantation of EGFR-driven GBM tumors (unpublished data) (Laramy et al., 2017). Based on literature review, a multi-targeted kinase inhibitor (ponatinib), an FDA-approved leukemia therapy, has

activities against PDGFR- $\alpha$  and RET, resulting in proteomic-guided drug selection for GBM6, one of the drug-resistant PDX GBM tumors (Laramy et al., 2017). Interestingly, depending on the characteristic of individual brain tumor, the same drug can lead to differential orthotopic efficacy. Ponatinib represents an interesting case because our previous preclinical study showed negative preclinical efficacy in an adult glioblastoma xenograft model (GBM6) (Laramy et al., 2017) whereas a positive outcome was observed in another brain tumor model, pediatric brain tumor xenograft (D-2159MG) (Keir et al., 2012). The tumor-dependent preclinical efficacy indicates potential influence of oncogenic make-up of GBM tumor on the blood-brain barrier (BBB) integrity (i.e., the extent of BBB leakiness). This can also subsequently lead to differential drug distribution and resultant orthotopic efficacy, warranting further in-depth assessment of brain penetration of ponatinib.

Free tissue drug concentration is often considered to be the therapeutically-relevant concentration, not the total drug concentration, based on the free drug hypothesis (Dubey et al., 1989; Hammarlund-Udenaes et al., 2008). At the blood-brain barrier (BBB), the net “clearance” or transport (i.e., influx vs. efflux at the BBB) governs delivery of free drug concentration from plasma to the brain. Drug distribution across the BBB is often restricted by the physical and biochemical barriers, such as tight junctions and efflux transporters, respectively. Tight junctions located between the BBB epithelial cells often prevent paracellular drug transport, and efflux transporters can actively reduce brain penetration of a compound (Abbott et al., 2006). Functional compensation by Bcrp and P-gp has been commonly reported for various compounds (Kodaira et al., 2010), including tyrosine kinase inhibitors (Agarwal et al., 2011a; Mittapalli et al., 2012; Oberoi et al., 2013). The triple knockout genotype (*Mdr1a/b*( $-/-$ )/*Bcrp1*( $-/-$ )) often exhibits a brain-to-plasma ratio that is higher than what would be expected from brain-to-plasma ratios observed in the *Bcrp1*( $-/-$ ) and *Mdr1a/b*( $-/-$ ) genotypes individually. Restricted drug distribution across the BBB and thus, subtherapeutic drug exposure at the GBM tumor-bearing brain, can lead to lack of efficacy even for a potent, highly lipophilic compound that would readily diffuse across the BBB cell layer if efflux transporters were not involved. Utilization of genetic knockout mice has been useful in determining the mechanism by which BBB efflux transporters limit CNS drug delivery, and in quantifying the rate and extent of CNS penetration of a compound (Agarwal et al., 2011a; Mittapalli et al., 2012; Oberoi et al., 2013).

A compound exhibiting a greater extent and duration of tissue exposure within the therapeutic window is assumed to elicit a superior therapeutic outcome at the targeted tissue site, such as a tumor (Suzuki et al., 2009). The BBB efflux transporters, however, may reduce both the extent and duration of drug exposure in the brain, which can lead to suboptimal efficacy in the tumor-bearing brain, despite the tumor-inhibitory potency of a compound. The present study aimed to quantitatively assess the influence of BBB efflux transporters on the extent and duration of CNS penetration of ponatinib. Experimental approaches to achieve this included in vivo studies utilizing the transporter knockout and wild-type mice, in conjunction with in vitro brain slices, to determine brain-specific volumes of distribution. Subsequently, quantitative analyses of CNS distribution employed non-compartmental analysis (NCA) and mechanistic modeling to quantify the extent and duration of CNS penetration of ponatinib by estimating several parameters, including the tissue transfer rate constants, brain-to-plasma ratios of both free and total drug ( $K_p$  or  $K_{p,uu}$ ), and mean transit time (MTT; the average time spent by ponatinib in the brain in a single passage). The results this study provides insight into the role of efflux transporters on the CNS penetration of ponatinib, and the implication of limited CNS delivery on the efficacy of ponatinib for GBM.

## MATERIALS AND METHODS

### Chemicals and reagents

Ponatinib hydrochloride (3-(2-imidazo[1,2-b]pyridazin-3-ylethynyl)-4-methyl-N-[4-[(4-methylpiperazin-1-yl)methyl]-3-(trifluoromethyl)phenyl]benzamide hydrochloride) was purchased from Chemietek (Indianapolis, IN), imatinib methanesulfonate (4-[(4-methylpiperazin-1-yl)methyl]-N-[4-methyl-3-[(4-pyridin-3-yl)pyrimidin-2-yl]amino]phenyl]benzamide) (>99% purity) from LC Laboratories (Woburn, MA), and [ $^2\text{H}_8$ ]-ponatinib (> 98% purity) from Alsachim SAS (Illkirch, France). Analytical-grade reagents were purchased from Thermo Fisher Scientific (Waltham, MA).

### Animals

Pharmacokinetic studies were conducted using Friend leukemia virus strain B (FVB) wild-type, *Bcrp1*( $-/-$ ), *Mdr1a/b*( $-/-$ ), and *Mdr1a/b*( $-/-$ )*Bcrp1*( $-/-$ ) mice (Taconic Biosciences, Inc., Germantown, NY). Animals were sourced from Taconic Biosciences, Inc. that has maintained animal colony following

the established procedures of breeding and back-crossing. Mice were bred and maintained in the American Association for the Accreditation of Laboratory Animal Care (AAALAC International) accredited animal housing facility at the Academic Health Center, University of Minnesota. Animals were housed in a standard 12-hour dark/light cycle with unlimited access to food and water. We used both female and male mice (50% male and 50% female) at the age of 8-14 weeks for in vivo pharmacokinetic studies. All animal experiments were approved by the University of Minnesota Institutional Animal Care and Use Committee (IACUC) and conducted in accordance with the Guide for the Care and Use of Laboratory Animals established by the U.S. National Institutes of Health (Bethesda, MD).

### Plasma and brain concentration-time profiles of ponatinib

The oral dose of 30 mg/kg, the optimal dose utilized in mice in several studies (Gozgit et al., 2012; De Falco et al., 2013), was selected in the current study to examine CNS distribution of ponatinib. This was the dose previously used to test in vivo efficacy of ponatinib in a patient-derived xenograft (PDX) GBM model (Laramy et al., 2017). Equivalent doses for the distribution and efficacy studies allow assessment of how the extent of brain penetration of ponatinib affects efficacy in the PDX GBM model. The dose was reduced to 3 mg/kg in the intravenous cohort to achieve similar exposures following the various modes of administration. The dosing formulation of ponatinib was prepared in a vehicle of DMSO:Tween80:Water (2:1:7) for intravenous administration, and 0.5% methylcellulose (% g/v) and 0.2% Tween 80 for oral administration on the day of the animal experiment. A single intravenous bolus dose (3 mg/kg) was administered to FVB wild-type and *Mdr1a/b*( $-/-$ )*Bcrp1*( $-/-$ ) mice via tail vein injection, followed by serial sacrifice at 0.25, 0.5, 1, 2, 4, 8 and 16 hours ( $N = 3-4$  at each time point). In a separate study, a single oral dose (30 mg/kg) of ponatinib was administered to FVB wild-type, *Bcrp1*( $-/-$ ), *Mdr1a/b*( $-/-$ ), and *Mdr1a/b*( $-/-$ )*Bcrp1*( $-/-$ ) mice via oral gavage followed by serial sacrifice at 0.5, 2, 4, 8, 12, 16 and 24 hours ( $N = 4$  at each time point). The mice were euthanized in a carbon dioxide chamber, followed by collection of blood via cardiac puncture and rapid surgical removal of the brain. The brain was rinsed with water and blotted to remove superficial meninges. Plasma was obtained by centrifuging the blood at 3500 rpm for 15 minutes at 4°C. Plasma and brain samples were stored at -80°C until LC-MS/MS analysis.

### **Steady-state brain distribution of ponatinib after intraperitoneal infusion**

A continuous intraperitoneal infusion was achieved by surgical implantation of an Alzet osmotic mini pump (model 1000D, DURECT corporation, Cupertino, CA) in the intraperitoneal cavity of FVB wild-type, *Bcrp1*( $-/-$ ), *Mdr1a/b*( $-/-$ ), and *Mdr1a/b*( $-/-$ )*Bcrp1*( $-/-$ ) mice as described previously (Agarwal et al., 2010). Ponatinib was dissolved in DMSO at a concentration of 40  $\mu\text{g}/\mu\text{L}$  and the solution was loaded into the mini pumps. The drug-loaded pumps were primed overnight by soaking them in sterile saline at 37°C. Mice were anesthetized with isoflurane, and following surgical implantation, the mice were infused with ponatinib at a constant rate of 1  $\mu\text{L}/\text{hr}$  (40  $\mu\text{g}/\text{hr}$ ) for 48 hours. Plasma and brain samples were collected and stored following the same procedure as described earlier.

### **Brain slice method to estimate the volume of distribution of free (unbound) drug in the brain**

Brain slice experiment was conducted as previously reported (Friden et al., 2009; Loryan et al., 2013) with the following modifications. Briefly, drug-native FVB wild-type animals were sacrificed under isoflurane anesthesia, and the brain was immediately harvested and immersed in ice-cold oxygenated, HEPES-buffered artificial fluid or extracellular fluid (aECF) (129 mM NaCl, 3 mM KCl, 1.4 mM  $\text{CaCl}_2$ , 1.2 mM  $\text{MgSO}_4$ , 0.4 mM  $\text{K}_2\text{HPO}_4$ , 25 mM HEPES, 10 mM glucose and 0.4 mM ascorbic acid). Two consecutive 300- $\mu\text{m}$  coronal sections were cut using a Vibratome at the cutting speed of 5 and amplitude (vibration) of 10 (Lancer TPI Vibratome Series 1000 Sectioning Microtome System, The Vibratome Company, St. Louis, MO). The slices were transferred into a 50 mm high, 90 mm diameter, flat-bottomed glass dish containing 200 nM ponatinib (10 mL) in aECF. A parafilm-covered beaker containing the aECF was gently infused with 100% oxygen. The beaker was gently shaken (UVP Multidizer hybridization oven) and incubated for 5 hours at 37°C with a rotation speed of 90 cycles/min. The slices were removed, dried on filter paper, and weighted in an Eppendorf tube. Each slice was individually homogenized with 9 volumes (w/v) of aECF buffer by vigorous vortexing. The 200  $\mu\text{L}$  of buffer was collected in an Eppendorf tube containing 200  $\mu\text{L}$  of blank brain homogenate (1:3 volumes of aECF buffer). The samples were stored at -80°C until LC-MS/MS analysis. The volume of distribution of free

drug ( $V_{u,brain}$ ) was calculated by the ratio of drug amount in the brain slice ( $A_{slice}$ ) to the buffer concentration ( $C_{buffer}$ ):

$$V_{u,brain} = \frac{A_{slice}}{C_{buffer}} \text{ (Equation 1a)}$$

$$V_{u,brain} = \frac{A_{slice} - V_i \cdot C_{buffer}}{C_{buffer} (1 - V_i)} \text{ (Equation 1b)}$$

The Equations 1a and 1b, are with or without, respectively, correction for the residual volume of buffer that can remain on the slice surface ( $V_i$ ). The literature value of  $V_i$  (mL/gram of brain slice) is 0.094 mL/g-brain (Kakee et al., 1996; Friden et al., 2009; Loryan et al., 2013). The free (unbound) brain-to-plasma concentration ratios ( $K_{p,uu}$ ) of ponatinib were calculated using the following equations adapted from Loryan et al. (2013). These equations incorporate the parameters, including the free drug fraction of ponatinib in plasma ( $f_{u,plasma} = 0.0023$ ) and brain homogenate ( $f_{u,brain} = 0.00029$ ).

$$\text{Free (unbound) brain-to-plasma concentration ratio} = K_{p,uu} = \frac{K_p}{V_{u,brain} \cdot f_{u,plasma}} \text{ (Equation 2a using } V_{u,brain})$$

$$\text{Free (unbound) brain-to-plasma concentration ratio} = K_{p,uu} = \frac{f_{u,brain}}{f_{u,plasma}} \cdot K_p \text{ (Equation 2b using } f_{u,brain})$$

### LC-MS/MS assay to measure ponatinib concentration

Total drug concentrations of ponatinib in plasma and brain specimens were measured using the LC-MS/MS method previously reported (Laramy et al., 2017). In summary, brain samples resulting from in vivo animal studies were homogenized with 3 tissue volumes of 5% bovine serum albumin (g/v) solution using a homogenizer (PowerGen 125; Thermo Fisher Scientific, Waltham, MA). Liquid-liquid extraction was performed for an aliquot of 25  $\mu$ L plasma or 50  $\mu$ L brain homogenate by adding 75 ng of internal standard (imatinib), 10 volumes of ice-cold ethyl acetate, and 5 volumes of 0.2 M sodium hydroxide (pH 13). The mixture was vortexed for 5 minutes, followed by centrifugation at 7500 rpm for 5 minutes (4°C). The organic layer was dried under nitrogen and reconstituted with 150  $\mu$ L of mobile phase (acetonitrile and 20 mM ammonium acetate with 0.05% formic acid), followed by centrifugation at 14000 rpm for 5 minutes (4°C). Five microliters of the sample was injected to the Zorbax XDB Eclipse C18 column (4.6 x 50 mm, 1.8  $\mu$ m; Agilent Technologies) for liquid chromatography. Gradient elution was performed to separate analyte for the samples resulting from all studies except of those from intravenous bolus dosing. For the samples from in vivo pharmacokinetic studies utilizing the intravenous bolus

dosing, a new isocratic method with a deuterated internal standard ( $[^2\text{H}_8]$ -ponatinib) was utilized in order to reduce the total run time to 7 minutes. For each of these LC-MS/MS methods, the calibration curve was sensitive and linear over the range of 0.4-2000 ng/mL (weighting factor of  $1/Y^2$ ) with coefficient of variation of less than 15%. All of the measured concentrations were within the range of the calibration curve.

## Pharmacokinetic data analysis

### 1) Non-compartmental analysis (NCA)

Plasma and brain concentration-time profiles resulting from administration of oral or intravenous bolus of ponatinib in different genotypes of mice were analyzed using Phoenix WinNonlin version 6.4 (Certara USA, Inc., Princeton, NJ). Non-compartmental analysis (NCA) was performed by trapezoidal rule integration to the last time point ( $\text{AUC}_{(0 \rightarrow t)}$ ) and to the time infinity including the extrapolated area ( $\text{AUC}_{(0 \rightarrow \infty)}$ ). The Phoenix NCA module also reported other parameters/metrics, such as clearance (CL or  $\text{CL}_{\text{apparent}}$ ), volume of distribution ( $V_d$  or  $V_{d,\text{apparent}}$ ), bioavailability (F), half-life, and  $C_{\text{max}}$ . Brain-to-plasma ratio of total drug (Kp) was calculated using three approaches for comparison: 1) the ratio of  $\text{AUC}_{(0 \rightarrow \infty)}$  of brain concentration-time profile ( $[\text{AUC}_{(0 \rightarrow \infty), \text{brain}}]$ ) to that of plasma concentration-time profile ( $[\text{AUC}_{(0 \rightarrow \infty), \text{plasma}}]$ ), 2) the ratio of steady-state brain concentration to steady-state plasma concentration, and 3) the ratio of the maximum brain concentration ( $C_{\text{max}, \text{brain}}$ ) to the corresponding plasma concentration ( $C_{p, \text{tss}}$ ) at that time point, since a “transient” steady state occurs at the time of  $C_{\text{max}, \text{brain}}$  (i.e.,  $T_{\text{max}, \text{brain}}$ ) (Oberoi et al., 2013). The free derivative of Kp ( $K_{p, \text{uu}}$ ) was calculated by multiplying the Kp value with the relative magnitude of free fraction of ponatinib in brain homogenate to plasma ( $f_{u, \text{brain}}/f_{u, \text{plasma}} = 0.00029/0.0023 = \text{approximately } 0.1$ ) (Laramy et al., 2017). A distribution advantage (DA) due to the lack of efflux transporters was quantitated by the ratio of  $K_{p, \text{knockout}}$  and  $K_{p, \text{wild-type}}$  (Oberoi et al., 2013; Parrish et al., 2015a; Vaidhyanathan et al., 2016) or  $K_{p, \text{uu}, \text{knockout}}$  and  $K_{p, \text{uu}, \text{wild-type}}$ . Using the calculated  $\text{AUC}_{(0 \rightarrow \infty)}$  values, the oral bioavailability (F) in the wild-type and *Mdr1a/b*(-/-)*Bcrp1*(-/-) mice was calculated using the following equation (Rowland and Tozer, 2011):

$$\text{Oral bioavailability (F)} = \left\{ \frac{[\text{AUC}_{(0 \rightarrow \infty), \text{plasma}}]_{\text{oral}}}{[\text{AUC}_{(0 \rightarrow \infty), \text{plasma}}]_{\text{IV}}} \right\} \left\{ \frac{\text{Dose}_{\text{IV}}}{\text{Dose}_{\text{oral}}} \right\} \quad (\text{Equation 3})$$

## 2) Compartmental analysis with a BBB model

A compartmental blood-brain barrier (BBB) model (Figure 1) was adapted from the literature (Wang and Welty, 1996; Hammarlund-Udenaes et al., 1997) and was implemented to quantitatively assess CNS distributional kinetics of ponatinib into and out of the brain. The model was fitted to the observed data (total plasma and brain concentration-time profiles) resulting from intravenous bolus and oral administration in the wild-type and genetic knockout mice. The assumptions for this model included: 1) Instantaneous equilibrium exists between the bound and free (unbound) drug in each compartment, 2) only free drug is available to move into and out of the brain at the BBB, and 3) the extent of drug binding in plasma and brain homogenate does not differ amongst the four genotypes. Nonlinear regression analysis for the BBB model was performed using SAAM II (version 2.3, The Epsilon Group, Charlottesville, VA).

The implementation of the BBB model was completed in two stages. The first stage involved describing the total plasma concentration with an open two-compartment model with drug elimination from the central compartment (Figure 1A). For the total plasma concentration resulting from intravenous or oral administration, the intercompartmental rate constants ( $K_{12}$  and  $K_{21}$ ), elimination rate constant from the central compartment ( $K_{10}$ ), volume of distribution in the central compartment ( $V_{\text{central}}$ ), and absorption rate constant ( $K_a$ ) were estimated. The terminal elimination rate constant ( $K_{\text{elim}}$ ) for drug elimination from the body was calculated by using the following equation (Gibaldi and Perrier, 1998):

$$k_{\text{elim}} = \frac{1}{2} \left[ (k_{12} + k_{21} + k_{10}) - \sqrt{(k_{12} + k_{21} + k_{10})^2 - 4k_{21} * k_{10}} \right] \text{ (Equation 4)}$$

The half-life and clearance ( $CL_{\text{systemic}}$ ) of ponatinib elimination from the systemic circulation or body were calculated using  $k_{\text{elim}}$ .

In the second stage, the forcing function, or the analytical solution to the open two-compartment model describing the total plasma concentration, was input into the compartmental BBB model, in order to estimate model parameters that describe the distribution of drug to the brain (Figure 1A).

The differential equation for the change in total brain concentration over time was the following:

$$V_{\text{brain}} * \frac{C_{\text{brain}}}{dt} = (k_{\text{in}} * V_{\text{central}}) * C_{\text{plasma}} - (k_{\text{out}} * V_{\text{brain}}) * C_{\text{brain}} \text{ (Equation 5)}$$

where  $V_{\text{brain}}$  is the volume of distribution of total drug in the brain,  $k_{\text{in}}$  and  $k_{\text{out}}$  are the tissue transfer rate constants into and out of the brain,  $V_{\text{central}}$  is the volume of distribution of total drug in the central compartment, and  $C_{\text{plasma}}$  and  $C_{\text{brain}}$  are the total drug concentrations in plasma and brain, respectively. After these parameters were estimated, the differential equation for the brain compartment was re-written to describe the movement of free drug as follows (Figure 1B):

$$V_{u,\text{brain}} * \frac{C_{u,\text{brain}}}{dt} = (k_{\text{in}} * V_{u,\text{central}}) * C_{u,\text{plasma}} - (k_{\text{out}} * V_{u,\text{brain}}) * C_{u,\text{brain}} \quad (\text{Equation 6})$$

where  $V_{u,\text{brain}}$  (mL/kg) is the volume of distribution of free drug in the brain,  $k_{\text{in}}$  and  $k_{\text{out}}$  ( $\text{hr}^{-1}$ ) are the tissue transfer rate constants into and out of the brain,  $V_{u,\text{central}}$  (mL/kg) is the volume of distribution of free drug in the central compartment, and  $C_{u,\text{plasma}}$  and  $C_{u,\text{brain}}$  are the free drug concentrations in plasma and brain, respectively.

Clearance of total or free drug into the brain ( $\text{CL}_{\text{in}}$  or  $\text{CL}_{u,\text{in}}$ ) and out of the brain ( $\text{CL}_{\text{out}}$  or  $\text{CL}_{u,\text{out}}$ ) can be expressed as a product of the rate constants and the corresponding volumes of distribution terms.

$$\text{CL}_{\text{in}} = k_{\text{in}} * V_{\text{central}} \quad \text{where } V_{\text{central}} = V_{u,\text{central}} * f_{u,\text{plasma}} \quad (\text{Equation 7a,b})$$

$$\text{CL}_{\text{out}} = k_{\text{out}} * V_{\text{brain}} \quad \text{where } V_{\text{brain}} = V_{u,\text{brain}} * f_{u,\text{brain}} \quad (\text{Equation 8a,b})$$

$$\text{CL}_{u,\text{in}} = k_{\text{in}} * V_{u,\text{central}} \quad (\text{Equation 9})$$

$$\text{CL}_{u,\text{out}} = k_{\text{out}} * V_{u,\text{brain}} \quad (\text{Equation 10})$$

The clearance terms,  $\text{CL}_{\text{in}}$  and  $\text{CL}_{u,\text{in}}$  (mL/hr/kg), represent the net drug clearance of total and free drug, respectively, from plasma to the brain. The clearance terms,  $\text{CL}_{\text{out}}$  and  $\text{CL}_{u,\text{out}}$  (mL/hr/kg), represent the sum of all drug clearances out of the brain resulting from efflux transport, drug metabolism, and flow processes.

During the second stage of model fitting procedure (BBB model), the rate constants ( $k_{\text{in}}$  and  $k_{\text{out}}$ ) were estimated, and other parameters ( $V_{\text{central}}$ ,  $V_{u,\text{central}}$ ,  $f_{u,\text{plasma}}$ ,  $V_{\text{brain}}$ ,  $V_{u,\text{brain}}$ ,  $f_{u,\text{brain}}$ ) were fixed. The  $V_{\text{central}}$  (1478.3 mL/kg of body weight) was obtained from the first stage of model fitting procedure (a two-compartment model describing the plasma concentration-time profiles). Given that the weight of brain constitutes approximately 1.8% of body weight in mice (Davies and Morris, 1993), the experimental value of  $V_{u,\text{brain}}$  (1.62 mL/g-brain from the brain slice method) was converted to 29.2 mL/kg of body weight and fixed in the BBB model (assuming 20% coefficient of variation). Using the free fraction values of

ponatinib in plasma ( $f_{u,plasma} = 0.0023$ ) and brain homogenate ( $f_{u,brain} = 0.00029$ ) that were previously reported (Laramy et al., 2017), the  $V_{u,central}$  ( $6.458 \times 10^5$  mL/kg, or 645.8 L/kg) and  $V_{brain}$  (0.0086 mL/kg) were calculated according to Equations 7b and 8b.

The duration of brain tissue exposure to ponatinib was quantitated with the mean transit time (MTT) using the following equation (Kong and Jusko, 1988).

$$\text{Mean transit time in the brain (MTT}_{\text{brain}}) = \frac{1}{k_{\text{out}}} \text{ (Equation 11)}$$

The BBB model-predicted brain-to-plasma ratio ( $K_{p,pred}$  or  $K_{p,uu,pred}$ ) was calculated by the ratio of model-predicted areas under the curve (ratio of  $AUC_{\text{brain}}$  to  $AUC_{\text{plasma}}$ ). These model-predicted  $K_p$  and  $K_{p,uu}$  values are expected to equal the ratio of clearance of total or free drug in and out of the brain.

$$K_{p,pred} = \frac{AUC_{(0 \rightarrow \infty), \text{total brain, predicted}}}{AUC_{(0 \rightarrow \infty), \text{total plasma, predicted}}} \cong \frac{\text{Total } C_{\text{max, brain}}}{\text{Corresponding total plasma concentration at that time } (C_{p, \text{tss}})} \cong \frac{CL_{\text{in}}}{CL_{\text{out}}} \text{ (Equation 12)}$$

$$K_{p,uu,pred} = \frac{AUC_{(0 \rightarrow \infty), \text{free brain, predicted}}}{AUC_{(0 \rightarrow \infty), \text{free plasma, predicted}}} \cong \frac{\text{Free } C_{\text{max, brain}}}{\text{Corresponding free plasma concentration at that time } (C_{p, \text{tss}})} \cong \frac{CL_{u, \text{in}}}{CL_{u, \text{out}}} \text{ (Equation 13)}$$

The predicted distribution advantage ( $DA_{\text{pred}}$ ) due to the lack of efflux transporters (the ratio of  $K_{p,pred, \text{knockout}}$  and  $K_{p,pred, \text{wild-type}}$ , or  $K_{p,uu,pred, \text{knockout}}$  and  $K_{p,uu,pred, \text{wild-type}}$ ) was also calculated using the model-predicted brain-to-plasma ratio values.

## Statistical analysis

All experimental data were presented as mean  $\pm$  standard deviation (S.D.) or standard error of the mean (S.E.M). The sample size in this study was determined from a power analysis assuming 20% variance and an alpha value of 0.05, where the power is about 80% to detect a true difference between the anticipated means (about 50%) in drug distribution studies. Two sample *t*-test or analysis of variance (ANOVA) with Bonferroni correction for multiple testing were used to compare the drug concentration or brain-to-plasma ratios ( $K_p$ ) of wild-type with each of the three other genotypes (*Bcrp1*( $-/-$ ), *Mdr1a/b*( $-/-$ ), and *Mdr1a/b*( $-/-$ )*Bcrp1*( $-/-$ )). Visual display of data and statistical tests were completed using GraphPad Prism (version 6; GraphPad Software, La Jolla, California, USA). A significance level at  $P < 0.05$  was applied to all statistical tests.

## RESULTS

### Plasma and brain concentration-time profiles of ponatinib following a single intravenous bolus dose

The total plasma and brain concentration-time profiles, and brain-to-plasma ratio profiles after administration of a single intravenous bolus dose of ponatinib (3 mg/kg) are presented in Figure 2. The total plasma concentration exhibited a bi-exponential decline with respect to time for both wild-type and *Mdr1a/b(-/-)Bcrp1(-/-)*, suggesting that a two-compartmental model may describe the systemic disposition of ponatinib. The terminal slopes in the total plasma and brain concentrations were similar (Figure 2A) regardless of the genotype, as reflected in the similar half-life calculated for plasma and brain concentration-time profiles (Table 1). In the wild-type, there was no consistent difference between the total plasma and brain concentrations at each time point ( $P > 0.05$ ), and the  $[AUC_{(0 \rightarrow \infty), \text{plasma}}]$  and  $[AUC_{(0 \rightarrow \infty), \text{brain}}]$  values were comparable (Table 1), resulting in the AUC-based Kp value of 1 (unity) for total drug concentrations (bound plus free). On other hand, the *Mdr1a/b(-/-)Bcrp1(-/-)* mice had total brain concentrations that were consistently higher than the plasma concentrations at all time points ( $* P < 0.05$ ; Figure 2B), resulting in an  $[AUC_{(0 \rightarrow \infty), \text{brain}}]$  that was 10 times higher than the  $[AUC_{(0 \rightarrow \infty), \text{plasma}}]$  (Table 1). The total brain ponatinib concentration showed a relative time delay in reaching the maximum concentration in *Mdr1a/b(-/-)Bcrp1(-/-)*, as the  $T_{\text{max, brain}}$  was 2 hours post dose in *Mdr1a/b(-/-)Bcrp1(-/-)* mice and 0.25 hour (15 minutes) in the wild-type. The brain-to-plasma ratio profile reached a plateau at an earlier time point (between 0.5 to 1 hour post dose) in the wild-type compared to the *Mdr1a/b(-/-)Bcrp1(-/-)* mice (approximately 2 hours post dose) (Figure 2C). At each time point, the brain-to-plasma ratio was consistently higher in the *Mdr1a/b(-/-)Bcrp1(-/-)* than the wild-type ( $* P < 0.05$ ). The brain-to-plasma ratio (AUC based Kp) was approximately 10-fold higher in *Mdr1a/b(-/-)Bcrp1(-/-)* mice than the wild-type, as reflected in the distribution advantage (DA) value of 10 (Figure 2C and Table 1). The Kp and DA values estimated using either  $AUC_{(0 \rightarrow t)}$  or  $AUC_{(0 \rightarrow \infty)}$  provided the similar results, as the percentage of extrapolated area between  $AUC_{(0 \rightarrow t)}$  or  $AUC_{(0 \rightarrow \infty)}$  was below 10%. The wild-type and *Mdr1a/b(-/-)Bcrp1(-/-)* had the systemic clearance of 12.3 and 11.1 mL/min/kg, volume of distribution ( $V_d$ ) of 3.2 and 3.4 L/kg, and plasma half-life of 3.0 and 3.5 hours, respectively, indicating no difference in the systemic elimination of ponatinib between the two genotypes. Further supporting that genotype has minimal

influence on systemic exposure of ponatinib, the two genotypes had comparable  $[AUC_{(0 \rightarrow \infty), \text{plasma}}]$  values and similar total plasma concentrations at all time points ( $P > 0.05$ ). However, unlike the total plasma concentrations, the total brain concentrations statistically differed between the two genotypes at all time points (\*  $P < 0.05$ ).

### Plasma and brain concentration-time profiles of ponatinib following a single oral dose

The total plasma and brain concentration-time profiles, and brain-to-plasma ratio profiles after administration of a single oral dose of ponatinib (30 mg/kg) in the wild-type were previously reported (Laramy et al., 2017). The present study compared the pharmacokinetic data resulting from the three genotypes that lack efflux transporters and those from the wild-type that were previously reported. In the wild-type, the total plasma and brain concentrations were similar at almost all time points ( $P > 0.05$  except of 0.5 hour time point) (Figure 3A), resulting in an  $[AUC_{(0 \rightarrow \infty), \text{brain}}] / [AUC_{(0 \rightarrow \infty), \text{plasma}}]$  ratio of 0.82 (Figure 4 and Table 2). The three other genotypes, including *Bcrp1*(-/-), *Mdr1a/b*(-/-), and *Mdr1a/b*(-/-)*Bcrp1*(-/-), had the AUC-based Kp values of 1.3, 3.6, and 14.2, respectively (Figure 4 and Table 2), as the total brain concentration differed from the plasma concentration at most of the time points (\*  $P < 0.05$ ) (Figure 3B, 3C, and 3D). The brain-to-plasma ratio profile reached a plateau at a relatively earlier time point (approximately 2 hour post dose) in the wild-type and *Bcrp1*(-/-) genotypes. A later plateau (4 to 8 hours post dose) was observed in the *Mdr1a/b*(-/-) and *Mdr1a/b*(-/-)*Bcrp1*(-/-) genotypes (Figure 4). The Kp values did not statistically differ between the wild-type and *Bcrp1*(-/-) ( $P > 0.05$ ). However, *Mdr1a/b*(-/-) and *Mdr1a/b*(-/-)*Bcrp1*(-/-) genotypes, respectively, had a significantly higher Kp value compared to the wild-type (\*  $P < 0.05$ ). The Kp value in the *Mdr1a/b*(-/-)*Bcrp1*(-/-) genotype was greater than the additive value of Kp in *Bcrp1*(-/-) and *Mdr1a/b*(-/-) genotypes (Figure 4 and Table 2), indicating functional compensation between P-gp and Bcrp in modulating brain distribution of ponatinib. The corresponding DA values (AUC based) were 1.6, 4.4, and 17.3, respectively (Table 2). Regardless of the methods of calculation (AUC or transient steady-state), the estimated values of Kp and DA values were consistent. The use of either  $AUC_{(0 \rightarrow t)}$  or  $AUC_{(0 \rightarrow \infty)}$  also led to the consistent values of Kp and DA, as the percentage of extrapolated areas between  $AUC_{(0 \rightarrow t)}$  and  $AUC_{(0 \rightarrow \infty)}$  was below 10%.

As observed upon intravenous bolus dosing, the total plasma concentrations at each time point ( $P > 0.05$ ), thus  $AUC_{(0 \rightarrow \infty), \text{plasma}}$  values, were comparable between the genotypes (Figure 3 and Table 2) upon oral dosing, suggesting lack of influence of P-gp and Bcrp on the systemic exposure of ponatinib. The calculated oral bioavailability of ponatinib (26.5% based on Equation 3) was identical between the wild-type and *Mdr1a/b*(-/-)*Bcrp1*(-/-) genotypes. The total brain concentration at each time point significantly differed between the wild-type and each of the three other genotypes (\*  $P < 0.05$ ). This demonstrates that while P-gp and Bcrp dramatically affect the targeted bioavailability of ponatinib to the brain, the efflux transporters do not influence oral bioavailability of ponatinib at the doses administered.

### Steady-state brain distribution of ponatinib after continuous intraperitoneal infusion

After continuous intraperitoneal infusion of 40 µg/hr of ponatinib for 48 hours, the steady-state total plasma and brain concentrations, and the corresponding total brain-to-plasma ratios were compared between the wild-type and each of the three genotypes (*Bcrp1*(-/-), *Mdr1a/b*(-/-), and *Mdr1a/b*(-/-)*Bcrp1*(-/-)) using ANOVA test with Bonferroni correction for multiple testing. The steady-state total plasma concentration of ponatinib did not differ between the wild-type and each of the three genotypes ( $P = 0.58$ ), whereas the total brain concentration differed between the wild-type and *Mdr1a/b*(-/-)*Bcrp1*(-/-) genotypes (\*  $P = 0.03$ ; Figure 5A). The steady-state total brain-to-plasma ratios were approximately 1.7, 3.7, and 15-fold higher in the *Bcrp1*(-/-), *Mdr1a/b*(-/-), and *Mdr1a/b*(-/-)*Bcrp1*(-/-) genotypes, respectively, compared to the wild-type (Figure 5B and Table 3) as reflected in the calculated DA values (Table 3). The *Mdr1a/b*(-/-)*Bcrp1*(-/-) genotype had a Kp value that was greater than the additive value of the Kp values of *Bcrp1*(-/-) and *Mdr1a/b*(-/-) genotypes. A data summary table (Table 4) compares the Kp estimates resulting from the different routes of administration (intravenous bolus, oral dosing or steady-state continuous intraperitoneal infusion) and methods of calculation (AUC, transient steady-state or steady-state based). The Kp estimates were consistent and robust, regardless of the route of administration and method of calculation.

### Ponatinib distribution in the brain based on the brain slice method

The brain slice method was conducted in order to determine the volume of distribution of free (unbound) ponatinib in the brain. The volume of distribution of free ponatinib ( $V_{u,brain}$ ) was estimated to be 1.62 mL/g·brain from Equation 1a. The same value of  $V_{u,brain}$  was obtained either with or without correction (Equations 1a and 1b, respectively) for the volume of buffer film that remains on the brain slice surface ( $V_i$ ). The estimated  $V_{u,brain}$  was greater than the physiological volume of total brain fluids (0.8 mL/g·brain) (Reinoso et al., 1997; Loryan et al., 2013). This indicates that ponatinib extensively binds to the non-fluid components of the brain, i.e., the parenchymal components or lysosomes. Based on the  $K_p$  estimate of ponatinib in the wild-type (i.e., 1.0) (Tables 1 and 2), the free (unbound) brain-to-plasma ratio ( $K_{p,uu}$ ) values were calculated to be 268.4 (using the  $V_{u,brain}$  parameter; Equation 2a) and 0.11 (using  $f_{u,brain}$ ; Equation 2b). Such drastic discrepancy in  $K_{p,uu}$  estimation depending on the equations used (Equation 2a versus 2b) could arise due to the pH partitioning of a basic drug (e.g., ponatinib and other anticancer drugs, such as paclitaxel and mitoxantrone) in its intra-brain distribution (Friden et al., 2011). The calculation of  $V_{u,brain}$  in the present study used the  $V_i$  value of 0.094 mL/g·brain slice. However, this  $V_i$  value was previously determined in Sprague-Dawley male rats (Kakee et al., 1996), not in the FVB wild-type mice, so that the possible interspecies differences in the  $V_i$  value could lead to a misleading value of  $V_{u,brain}$ . Therefore, for the assessment of brain penetration of ponatinib, the  $K_{p,uu}$  of 0.11 (based on Equation 2b) was assumed.

### **Equilibration of total and free ponatinib across the blood-brain barrier (BBB): Insight from a BBB model**

For the implementation of a BBB model, the total plasma concentrations were pooled across all genotypes following either a single intravenous bolus or oral dose, given that we found essentially the same concentration-time profiles, bioavailability and systemic exposure (i.e.,  $AUC_{(0 \rightarrow \infty), plasma}$ ) of ponatinib amongst the genotypes. The total plasma concentration-time profiles were best described by an open two-compartmental model, and the resultant estimates of pharmacokinetic parameters are shown in Table 5. The predicted plasma concentration-time profiles (resulting from the naïve-pooled analysis) described the observed (total drug) plasma concentration-time profiles as shown in Figures 6A, 6B, and 7. The volume of distribution of ponatinib in the central compartment was estimated to be 1478.3 mL/kg,

inter-compartmental rate constants ( $k_{21}$  and  $k_{12}$ ) were  $2.34 \text{ hr}^{-1}$  and  $2.15 \text{ hr}^{-1}$ , respectively, elimination rate constant from the central compartment ( $k_{10}$ ) was  $0.47 \text{ hr}^{-1}$ , and absorption rate constant ( $k_a$ ) was  $0.28 \text{ hr}^{-1}$ . All parameter estimates had a coefficient of variation (CV) of less than 20% (Table 5). Using these estimated parameters, the volume of distribution of unbound (free) drug in the central compartment ( $V_{u, \text{central}} = 645.8 \text{ L/kg}$  using Equation 7b), terminal elimination rate constant from the body ( $k_{\text{elim}} = 0.21 \text{ hr}^{-1}$  using Equation 4), clearance of ponatinib from systemic circulation ( $\text{CL}_{\text{systemic}} = 310.4 \text{ mL/hr/kg}$ ), and half-life (3.3 hr) for ponatinib elimination from systemic circulation were calculated (Table 5).

The BBB model (Figure 1) described the observed plasma and brain concentration-time data well, as displayed in Figures 6 and 7. Each genotype's individual total plasma concentration-time profile visually matches the model-predicted plasma concentration-time profile resulting from fitting the model to the naïve-pooled plasma data from all genotypes (Figures 6 and 7). Upon initial fitting of the BBB model, the tissue transfer rate constant of ponatinib into the brain ( $k_{\text{in}}$ ) of each genotype was similar to the  $k_{\text{in}}$  of the *Mdr1a/b(-/-)Bcrp1(-/-)* genotype. Therefore, the  $k_{\text{in}}$  value, which describes the influx processes at the BBB for ponatinib, was assumed to be the same across the four genotypes, and the  $k_{\text{in}}$  estimate from *Mdr1a/b(-/-)Bcrp1(-/-)* genotype was subsequently used and fixed for the three other genotypes for the remaining model fitting procedures to make the fitting routines more tractable. The resultant pharmacokinetic parameter estimates from the BBB model are displayed in Table 6.

Based on the implemented BBB model, each genotype had a considerably different tissue transfer rate constant out of the brain (brain exit rate constant, or  $k_{\text{out}}$ ) and clearances out of the brain ( $\text{CL}_{\text{out}}$  and  $\text{CL}_{u, \text{out}}$ ) for ponatinib, regardless of the route of administration (intravenous bolus or oral). Clearances of ponatinib out of the brain ( $\text{CL}_{\text{out}}$  and  $\text{CL}_{u, \text{out}}$ ) were reduced by 1.5, 4.2, and approximately 19-fold in *Bcrp1(-/-)*, *Mdr1a/b(-/-)*, and *Mdr1a/b(-/-)Bcrp1(-/-)*, respectively (Table 7). Consistent with the magnitude differences in the clearances out of the brain ( $\text{CL}_{\text{out}}$  and  $\text{CL}_{u, \text{out}}$ ), the estimated  $k_{\text{out}}$  values were the greatest in the wild-type and lowest in the *Mdr1a/b(-/-)Bcrp1(-/-)* genotype. Likewise, the mean transit time of ponatinib in the brain ( $\text{MTT}_{\text{brain}}$ ; calculated by Equation 11) was the shortest in the wild-type (approximately 5 minutes), followed by *Bcrp1(-/-)*, *Mdr1a/b(-/-)*, and longest in *Mdr1a/b(-/-)Bcrp1(-/-)* genotype (approximately 1.5 hours). These values indicate that transporter-mediated drug

efflux at the BBB can significantly reduce the therapeutic exposure time of ponatinib in the brain (Table 6).

Using the pharmacokinetic parameters estimated from the BBB model, and the resultant metrics (predicted AUCs), the total and free brain-to-plasma ratios ( $K_{p,pred}$  and  $K_{p,uu,pred}$ ), and distribution advantages ( $DA_{pred}$ ) were calculated. These values are presented in Table 7. The  $K_{p,pred}$ , or  $CL_{in}/CL_{out}$ , resulting from the compartmental analysis (BBB model) (Table 7) closely matched the observed  $K_p$  from the non-compartmental analysis (Tables 1-4). Likewise, the resultant free derivative of  $K_p$  (i.e.,  $K_{p,uu}$ ) from the non-compartmental analysis also closely aligned with the ratio of  $CL_{u,in}$  to  $CL_{u,out}$ , as anticipated. Therefore, the model-predicted  $K_p$ ,  $K_{p,uu}$  and  $DA$  values ( $K_{p,pred}$ ,  $K_{p,uu,pred}$ , and  $DA_{pred}$ ) were consistent with the non-compartmental analyses, regardless of the calculation method (AUC, transient steady state, and clearance based), as shown in Table 7. These predicted values were similar to the observed (experimental) data (Tables 1-4), supporting that the model-related assumptions were reasonable, and the data were well-characterized by the BBB model.

## DISCUSSION

Functionally cooperative drug transport by the blood-brain barrier (BBB) efflux transporters has been previously reported for several tyrosine kinase inhibitors with important implications of such restricted brain delivery having a negative impact on efficacy (Parrish et al., 2015b). Consistent with our recent publication that reported restricted orthotopic efficacy of ponatinib in a patient-derived xenograft (PDX) GBM model (Laramy et al., 2017), the present study showed the transporter-mediated drug efflux at the BBB, which supports its contribution to impaired free drug delivery of ponatinib to the brain. The distribution advantage due to the absence of both P-gp and Bcrp transporter activities was greater when compared to the absence of a single transporter. This suggests that ponatinib is a dual substrate of P-gp and Bcrp, where these two transporters functionally cooperate to restrict brain distribution of ponatinib (Agarwal et al., 2011a; Agarwal et al., 2011b). Eliminating the gatekeeper functions of these efflux transporters decreased the tissue transfer rate constant (brain exit rate constant, or  $k_{out}$ ) and clearance of ponatinib out of the brain ( $CL_{out}$  and  $CL_{u,out}$ ), resulting in a greater tissue exposure ( $AUC_{brain}$ ) as well as a greater mean transit time (MTT), or therapeutic exposure time in the brain in the efflux deficient mice.

The magnitude of differences in the transport of ponatinib out of the brain between the four genotypes (i.e., brain exit rate constants and clearances out of the brain) can be described by the  $K_p$  and  $K_{p,uu}$  estimates. However, the clearance and  $K_p$  estimates based on total drug can be misleading because this does not consider free (active) drug concentration (Laramy et al., 2017). A  $K_p$  value near unity, as seen with ponatinib, does not always indicate that drug in plasma moves effectively across the BBB, as the  $K_p$  values can be confounded by the relative magnitude of drug binding affinities between plasma and brain. Instead, only free drug is available to move across the BBB, so that assessment of BBB penetration needs to utilize the parameters that reflect the movement of free drug, including  $K_p$  of free drug ( $K_{p,uu}$ ) and volume of distribution of free drug in the brain ( $V_{u,brain}$ ). These results are consistent with a previous publication that reported compromised efficacy of ponatinib in the patient-derived xenograft model (PDX) of glioblastoma due to the heterogeneous tissue binding and drug distribution into the intracranial tumor (Laramy et al., 2017). This discrepancy between  $K_p$  and  $K_{p,uu}$  highlights the importance of considering the relative drug binding in plasma and brain, as a high  $K_p$ , i.e., near unity, can misrepresent the extent of brain delivery of active compound, and therefore may not accurately predict delivery of an efficacious drug concentration. The ratio of free fraction in brain homogenate to that in plasma ( $f_{u,brain}/f_{u,plasma}$ ) matched the distribution advantage ( $K_{p,knockout}/K_{p,wild-type}$ ), which is consistent with a previous report that assessed such correlation for the purpose of predicting the extent of CNS penetration of investigational compounds (Kalvass et al., 2007). The extent of brain penetration ( $K_{p,uu}$ ) of a compound in the *Mdr1a/b(-/-)Bcrp1(-/-)* genotype will presumably equal unity (1), if all transporter-mediated efflux was absent, and the clearances into and out of the brain were equivalent. However, the observed  $K_{p,uu}$  values were slightly greater than 1, ranging from 1.1 to 1.7, in the *Mdr1a/b(-/-)Bcrp1(-/-)* mice. While experimental errors could also lead to a  $K_{p,uu}$  of greater than 1, the existence of a weak influx system that transports ponatinib into the brain could also lead to this result. In light of this  $K_{p,uu}$  in the triple knockout mice, the substrate status of ponatinib regarding possible BBB uptake transporters is of interest. These transporters may include various organic anion and especially cation transport systems, and nutrient influx transports, such as the amino acid influx systems (Ohtsuki and Terasaki, 2007). It is known that influx systems can influence the extent of partitioning of free drug across the BBB.

Further investigation of such influx mechanism is necessary to determine whether this possible small influx component of ponatinib can affect the resultant efficacy in a tumor-bearing brain.

The use of transporter knockout mice has been useful in elucidating functionally cooperative transporter-mediated drug efflux at the BBB for investigational compounds. The total brain-to-plasma ratio ( $K_p$ ) in the triple knockout mice (*Mdr1a/b*( $-/-$ )*Bcrp1*( $-/-$ )) had greater than additive increase in the  $K_p$  in a single knockout mice missing either *Bcrp* or P-glycoprotein, regardless of the route of administration and analysis approaches (i.e., non-compartmental and compartmental analyses). This suggests that the absence of one efflux transporter leads to functional compensation by another efflux transporter for ponatinib, as previously described for many compounds in the literature (Kodaira et al., 2010). Such functional cooperation of BBB efflux transporters is not accompanied by compensatory changes in the expression of P-gp and *Bcrp* in the isolated brain capillaries of the four genotypes—wild-type, *Bcrp1*( $-/-$ ), *Mdr1a/b*( $-/-$ ), and *Mdr1a/b*( $-/-$ )*Bcrp1*( $-/-$ ) according to a previous quantitative proteomic study (Agarwal et al., 2012). This proteomic study also reported that the quantitative expression level of P-gp (*Mdr1a/b*) is approximately 4.6-fold higher than that of *Bcrp* in the brain capillary endothelial cells isolated from wild-type, *Bcrp1*( $-/-$ ), and *Mdr1a/b*( $-/-$ )*Bcrp1*( $-/-$ ) mice. Therefore, genetic deletion of P-gp would lead to a higher brain-to-plasma ratio ( $K_p$  or  $K_{p,uu}$ ) than that of *Bcrp*, especially when the drug transport capacity (relative expression levels) of these efflux transporters, not differences in relative affinity (binding affinity to P-gp versus *Bcrp*), dictates the transporter-mediated efflux. Ponatinib had a higher brain-to-plasma ratio in the absence of P-gp (*Mdr1a/b*( $-/-$ )) as compared to *Bcrp* (*Bcrp1*( $-/-$ )) in the present study. This suggests that functional capacity, in relation to cooperative efflux of P-gp and *Bcrp*, drives transporter-mediated efflux of ponatinib at the BBB.

Efficient net efflux of a drug at the BBB will lead to a free brain-to-plasma ratio ( $K_{p,uu}$ ) below 1, where the efflux capability exceeds influx of a free drug at the BBB ( $CL_{u,in} < CL_{u,out}$ ). Most tyrosine kinase inhibitors that have been examined for the treatment of brain tumor have total and free brain-to-plasma ratios below 1 (Ballard et al., 2016; Heffron, 2016). Other processes in the brain, including drug metabolism within the brain and bulk flow (extracellular fluid drainage), may contribute to clearance of a drug out of the brain, but transporter-mediated efflux is often a key main contributor of such elimination mechanisms relative to other processes. The unbound drug concentration in plasma drives the

movement of drug across the BBB into the brain, but the relative difference between the brain exit rate constant ( $k_{out}$ ) and terminal rate constant for drug elimination from the body ( $k_{elim}$ ) determines the effective half-life of drug in the brain. The present study showed that the brain exit rate constant ( $k_{out}$ ) was greater than the terminal rate constant out of the body ( $k_{elim}$ ) for ponatinib, which will influence the time-dependence of drug partitioning into the brain (Tables 5 and 6).

In conclusion, this study showed that the two major efflux transporters, P-glycoprotein (P-gp) and breast cancer resistance protein (Bcrp), cooperate to modulate the brain exposure of ponatinib without affecting systemic exposure to ponatinib. Genetically-modified mice lacking both P-gp and Bcrp displayed a brain-to-plasma ratio that was higher than what would be anticipated from brain-to-plasma ratios in the single knockout genotype (*Mdr1a/b*( $-/-$ ) or *Bcrp1*( $-/-$ )), indicating functionally cooperative transport of ponatinib out of the brain. The compartmental and non-compartmental analyses resulted in similar parameter estimates describing the extent of brain penetration, and the compartmental BBB model described the observed data well (plasma and brain concentration-time profiles) providing insight on transport of ponatinib across the BBB. Transporter-mediated efflux transport at the BBB reduced the extent of brain penetration (both  $K_p$  and  $K_{p,uu}$ ) of ponatinib, and such transport mechanism further compromised the therapeutic exposure time (mean transit time) in the brain. Ponatinib brain distribution is an exemplary case to appreciate how drug binding may influence efficacy and how the total  $K_p$  (brain-to-plasma ratio) may be misleading. Combined with the previous data regarding heterogeneous binding and drug distribution in the intracranial tumor (Laramy et al., 2017), transporter-mediated efflux of ponatinib at the BBB further compromises its therapeutic potential for the treatment of glioblastoma (GBM).

## ACKNOWLEDGEMENTS

The authors thank Jim Fisher, Clinical Pharmacology Analytical Laboratory, University of Minnesota, for his support in the development of the LC-MS/MS assay for ponatinib, and David Hottman, a graduate student in the department of Experimental and Clinical Pharmacology, University of Minnesota, for hands-on demonstration on how to use a Vibratome.

## **AUTHORSHIP CONTRIBUTIONS**

Participated in research design: Laramy, Kim, Parrish, Sarkaria, and Elmquist

Conducted experiments: Laramy, Kim, and Parrish

Conducted data analysis: Laramy, Kim, and Elmquist

Contributed new reagents or analytic tools: Laramy

Wrote or contributed to the writing of the manuscript: Laramy, Kim, Parrish, Sarkaria, and Elmquist

## REFERENCES

- Abbott NJ, Ronnback L and Hansson E (2006) Astrocyte-endothelial interactions at the blood-brain barrier. *Nat Rev Neurosci* **7**:41-53.
- Agarwal S, Hartz AM, Elmquist WF and Bauer B (2011a) Breast cancer resistance protein and P-glycoprotein in brain cancer: two gatekeepers team up. *Curr Pharm Des* **17**:2793-2802.
- Agarwal S, Sane R, Gallardo JL, Ohlfest JR and Elmquist WF (2010) Distribution of gefitinib to the brain is limited by P-glycoprotein (ABCB1) and breast cancer resistance protein (ABCG2)-mediated active efflux. *J Pharmacol Exp Ther* **334**:147-155.
- Agarwal S, Sane R, Oberoi R, Ohlfest JR and Elmquist WF (2011b) Delivery of molecularly targeted therapy to malignant glioma, a disease of the whole brain. *Expert Rev Mol Med* **13**:e17.
- Agarwal S, Uchida Y, Mittapalli RK, Sane R, Terasaki T and Elmquist WF (2012) Quantitative proteomics of transporter expression in brain capillary endothelial cells isolated from P-glycoprotein (P-gp), breast cancer resistance protein (Bcrp), and P-gp/Bcrp knockout mice. *Drug Metab Dispos* **40**:1164-1169.
- Ballard P, Yates JW, Yang Z, Kim DW, Yang JC, Cantarini M, Pickup K, Jordan A, Hickey M, Grist M, Box M, Johnstrom P, Varnas K, Malmquist J, Thress KS, Janne PA and Cross D (2016) Preclinical Comparison of Osimertinib with Other EGFR-TKIs in EGFR-Mutant NSCLC Brain Metastases Models, and Early Evidence of Clinical Brain Metastases Activity. *Clin Cancer Res* **22**:5130-5140.
- Davies B and Morris T (1993) Physiological parameters in laboratory animals and humans. *Pharm Res* **10**:1093-1095.
- De Falco V, Buonocore P, Muthu M, Torregrossa L, Basolo F, Billaud M, Gozgit JM, Carlomagno F and Santoro M (2013) Ponatinib (AP24534) is a novel potent inhibitor of oncogenic RET mutants associated with thyroid cancer. *J Clin Endocrinol Metab* **98**:E811-819.
- De Witt Hamer PC (2010) Small molecule kinase inhibitors in glioblastoma: a systematic review of clinical studies. *Neuro Oncol* **12**:304-316.
- Dubey RK, McAllister CB, Inoue M and Wilkinson GR (1989) Plasma binding and transport of diazepam across the blood-brain barrier. No evidence for in vivo enhanced dissociation. *J Clin Invest* **84**:1155-1159.

- Friden M, Bergstrom F, Wan H, Rehngren M, Ahlin G, Hammarlund-Udenaes M and Bredberg U (2011) Measurement of unbound drug exposure in brain: modeling of pH partitioning explains diverging results between the brain slice and brain homogenate methods. *Drug Metab Dispos* **39**:353-362.
- Friden M, Ducrozet F, Middleton B, Antonsson M, Bredberg U and Hammarlund-Udenaes M (2009) Development of a high-throughput brain slice method for studying drug distribution in the central nervous system. *Drug Metab Dispos* **37**:1226-1233.
- Gibaldi M and Perrier D (1998) *Pharmacokinetics*. Marcel Dekker, Inc., New York.
- Gozgit JM, Wong MJ, Moran L, Wardwell S, Mohemmad QK, Narasimhan NI, Shakespeare WC, Wang F, Clackson T and Rivera VM (2012) Ponatinib (AP24534), a multitargeted pan-FGFR inhibitor with activity in multiple FGFR-amplified or mutated cancer models. *Mol Cancer Ther* **11**:690-699.
- Hammarlund-Udenaes M, Friden M, Syvanen S and Gupta A (2008) On the rate and extent of drug delivery to the brain. *Pharm Res* **25**:1737-1750.
- Hammarlund-Udenaes M, Paalzow LK and de Lange EC (1997) Drug equilibration across the blood-brain barrier--pharmacokinetic considerations based on the microdialysis method. *Pharm Res* **14**:128-134.
- Heffron TP (2016) Small Molecule Kinase Inhibitors for the Treatment of Brain Cancer. *J Med Chem* **59**:10030-10066.
- Kakee A, Terasaki T and Sugiyama Y (1996) Brain efflux index as a novel method of analyzing efflux transport at the blood-brain barrier. *J Pharmacol Exp Ther* **277**:1550-1559.
- Kalvass JC, Maurer TS and Pollack GM (2007) Use of plasma and brain unbound fractions to assess the extent of brain distribution of 34 drugs: comparison of unbound concentration ratios to in vivo p-glycoprotein efflux ratios. *Drug Metab Dispos* **35**:660-666.
- Keir S, Saling J, Roskoski M, Friedman H and Bigner D (2012) Efficacy of combination therapy with ponatinib (AP24534) +/- bevacizumab against pediatric glioblastoma. *Neuro Oncol* **14**:i56–i68.
- Kodaira H, Kusuhara H, Ushiki J, Fuse E and Sugiyama Y (2010) Kinetic analysis of the cooperation of P-glycoprotein (P-gp/Abcb1) and breast cancer resistance protein (Bcrp/Abcg2) in limiting the brain and testis penetration of erlotinib, flavopiridol, and mitoxantrone. *J Pharmacol Exp Ther* **333**:788-796.

- Kong AN and Jusko WJ (1988) Definitions and applications of mean transit and residence times in reference to the two-compartment mammillary plasma clearance model. *J Pharm Sci* **77**:157-165.
- Laramy JK, Kim M, Gupta SK, Parrish KE, Zhang S, Bakken KK, Carlson BL, Mladek AC, Ma DJ, Sarkaria JN and Elmquist WF (2017) Heterogeneous Binding and Central Nervous System Distribution of the Multitargeted Kinase Inhibitor Ponatinib Restrict Orthotopic Efficacy in a Patient-Derived Xenograft Model of Glioblastoma. *J Pharmacol Exp Ther* **363**:136-147.
- Loryan I, Friden M and Hammarlund-Udenaes M (2013) The brain slice method for studying drug distribution in the CNS. *Fluids Barriers CNS* **10**:6.
- Mittapalli RK, Vaidhyanathan S, Sane R and Elmquist WF (2012) Impact of P-glycoprotein (ABCB1) and breast cancer resistance protein (ABCG2) on the brain distribution of a novel BRAF inhibitor: vemurafenib (PLX4032). *J Pharmacol Exp Ther* **342**:33-40.
- Oberoi RK, Mittapalli RK and Elmquist WF (2013) Pharmacokinetic assessment of efflux transport in sunitinib distribution to the brain. *J Pharmacol Exp Ther* **347**:755-764.
- Ohtsuki S and Terasaki T (2007) Contribution of carrier-mediated transport systems to the blood-brain barrier as a supporting and protecting interface for the brain; importance for CNS drug discovery and development. *Pharm Res* **24**:1745-1758.
- Ostrom QT, Gittleman H, Xu J, Kromer C, Wolinsky Y, Kruchko C and Barnholtz-Sloan JS (2016) CBTRUS Statistical Report: Primary Brain and Other Central Nervous System Tumors Diagnosed in the United States in 2009-2013. *Neuro Oncol* **18**:v1-v75.
- Parrish KE, Cen L, Murray J, Calligaris D, Kizilbash S, Mittapalli RK, Carlson BL, Schroeder MA, Sludden J, Boddy AV, Agar NY, Curtin NJ, Elmquist WF and Sarkaria JN (2015a) Efficacy of PARP Inhibitor Rucaparib in Orthotopic Glioblastoma Xenografts Is Limited by Ineffective Drug Penetration into the Central Nervous System. *Mol Cancer Ther* **14**:2735-2743.
- Parrish KE, Pokorny J, Mittapalli RK, Bakken K, Sarkaria JN and Elmquist WF (2015b) Efflux transporters at the blood-brain barrier limit delivery and efficacy of cyclin-dependent kinase 4/6 inhibitor palbociclib (PD-0332991) in an orthotopic brain tumor model. *J Pharmacol Exp Ther* **355**:264-271.

- Reinoso RF, Telfer BA and Rowland M (1997) Tissue water content in rats measured by desiccation. *J Pharmacol Toxicol Methods* **38**:87-92.
- Rowland M and Tozer TN (2011) *Clinical pharmacokinetics and pharmacodynamics: concepts and applications*. Wolters Kluwer Health/Lippincott William & Wilkins, Philadelphia.
- Suzuki Y, Tanaka K, Negishi D, Shimizu M, Yoshida Y, Hashimoto T and Yamazaki H (2009) Pharmacokinetic investigation of increased efficacy against malignant gliomas of carboplatin combined with hyperbaric oxygenation. *Neurol Med Chir (Tokyo)* **49**:193-197; discussion 197.
- Vaidhyanathan S, Wilken-Resman B, Ma DJ, Parrish KE, Mittapalli RK, Carlson BL, Sarkaria JN and Elmquist WF (2016) Factors Influencing the Central Nervous System Distribution of a Novel Phosphoinositide 3-Kinase/Mammalian Target of Rapamycin Inhibitor GSK2126458: Implications for Overcoming Resistance with Combination Therapy for Melanoma Brain Metastases. *J Pharmacol Exp Ther* **356**:251-259.
- Wang Y and Welty DF (1996) The simultaneous estimation of the influx and efflux blood-brain barrier permeabilities of gabapentin using a microdialysis-pharmacokinetic approach. *Pharm Res* **13**:398-403.

## FOOTNOTES

This work was supported by the National Institutes of Health [Grants RO1 CA138437, RO1 NS077921, U54 CA210180, and P50 CA108961]. Janice K. Laramy was supported by the Edward G. Rippie, Rory P. Remmel and Cheryl L. Zimmerman in Drug Metabolism and Pharmacokinetics, and American Foundation for Pharmaceutical Education (AFPE) Pre-Doctoral Fellowships. This work was presented, in part, in Janice K. Laramy's doctoral dissertation as follows: Permeability, binding and distributional kinetics of ponatinib, a multi-kinase inhibitor: implications for the treatment of brain tumors. Doctoral dissertation, University of Minnesota, Minneapolis, Minnesota.

## LEGENDS FOR FIGURES

**Figure 1.** A compartmental blood-brain barrier (BBB) model was adapted from literature (Wang and Welty, 1996; Hammarlund-Udenaes et al., 1997) in order to describe drug movement between plasma and brain tissue after administration of a single intravenous bolus or oral dose: (A) An open two-compartment model described the total drug concentration-time profile in plasma with the parameters ( $k_{12}$ ,  $k_{21}$ ,  $k_{10}$ , and/or  $k_a$ ) that were used to generate a forcing function. The forcing function was subsequently input and used in the BBB model, which simultaneously described the total plasma and brain concentration-time profiles ( $C_{\text{plasma}}$  and  $C_{\text{brain}}$ ). (B) A BBB model for free (unbound) drug in plasma and brain compartments.

$X_{\text{peripheral}}$ , total drug amount in the peripheral compartment

$V_{\text{central}}$ , volume of distribution of total drug in the central compartment

$V_{u,\text{central}}$ , volume of distribution of free (unbound) drug in the central compartment

$V_{u,\text{brain}}$ , volume of distribution of free (unbound) drug in the brain compartment

$K_{10}$ , elimination rate constant from the central compartment

$K_{12}$  and  $K_{21}$ , intercompartmental transfer rate constants

$K_{\text{elim}}$ , terminal rate constant (elimination from the body) from Equation 4

$K_a$ , absorption rate constant after oral dosing

$k_{\text{in}}$ , tissue transfer rate constant into the brain

$k_{\text{out}}$ , tissue transfer rate constant out of the brain (brain exit rate constant)

$C_{\text{plasma}}$  and  $C_{u,\text{plasma}}$ , total and free plasma concentration

$C_{\text{brain}}$  and  $C_{u,\text{brain}}$ , total and free brain concentration

**Figure 2.** Total plasma (solid line with square) concentration and brain (dashed line with circle) concentration in (A) wild-type mice, (B) *Mdr1a/b*(-/-)*Bcrp1*(-/-) mice, and (C) brain-to-plasma ratio time course of ponatinib after administration of a single intravenous bolus (3 mg/kg) in FVB wild-type and *Mdr1a/b*(-/-)*Bcrp1*(-/-) mice ( $N = 3-4$  at each time point). Data are presented as mean  $\pm$  standard deviation (S.D.). The two genotypes had similar total plasma concentrations at all time points ( $P > 0.05$ ), whereas the total brain concentrations differed (\*  $P < 0.05$ ). The total brain concentrations were

consistently higher than the total plasma concentrations at all time points in *Mdr1a/b*( $-/-$ )*Bcrp1*( $-/-$ ) mice (\*  $P < 0.05$ ) unlike the wild-type ( $P > 0.05$ ). The *Mdr1a/b*( $-/-$ )*Bcrp1*( $-/-$ ) genotype had the brain-to-plasma ratio that was greater than the wild-type at each time point (\*  $P < 0.05$ ).

**Figure 3.** Total plasma (solid line with square) and brain (dashed line with circle) concentration-time profiles after administration of a single oral dose (30 mg/kg) of ponatinib in (A) FVB wild-type, (B) *Bcrp1*( $-/-$ ), (C) *Mdr1a/b*( $-/-$ ), and (D) *Mdr1a/b*( $-/-$ )*Bcrp1*( $-/-$ ) mice ( $N = 4$  at each time point). Data are presented as mean  $\pm$  standard deviation (S.D.). Data for the wild-type were previously reported (Laramy et al., 2017) and included in this present study, in order to compare the wild-type with the three other genotypes that lack efflux transporter(s). The four genotypes had similar total plasma concentrations at all time points ( $P > 0.05$ ), whereas the total brain concentrations differed (\*  $P < 0.05$ ). The total brain concentrations were higher than the total plasma concentrations at most of the time points in each of the three genetic knockout mice (\*  $P < 0.05$ ) unlike the wild-type ( $P > 0.05$ ).

**Figure 4.** Total brain-to-plasma ratio profiles after administration of a single oral dose (30 mg/kg) in FVB wild-type, *Bcrp1*( $-/-$ ), *Mdr1a/b*( $-/-$ ), and *Mdr1a/b*( $-/-$ )*Bcrp1*( $-/-$ ) mice ( $N = 4$  at each time point). Data are presented as mean  $\pm$  standard deviation (S.D.). Data for the wild-type were previously reported (Laramy et al., 2017) and included in this present study, in order to compare the wild-type with the three other genotypes that lack efflux transporter(s). The Kp values did not statistically differ between the wild-type and *Bcrp1*( $-/-$ ) ( $P > 0.05$ ). However, *Mdr1a/b*( $-/-$ ) and *Mdr1a/b*( $-/-$ )*Bcrp1*( $-/-$ ) genotypes, respectively, had a significantly higher Kp value compared to the wild-type (\*  $P < 0.05$ ).

**Figure 5.** (A) Total steady-state plasma and brain concentrations, and (B) corresponding total steady-state brain-to-plasma ratios of ponatinib after continuous intraperitoneal infusion (40  $\mu$ g/hr) for 48 hours in FVB wild-type, *Bcrp1*( $-/-$ ), *Mdr1a/b*( $-/-$ ), and *Mdr1a/b*( $-/-$ )*Bcrp1*( $-/-$ ) mice ( $N = 4$  in each genotype) (\*  $P < 0.05$ ). Data are presented as mean  $\pm$  standard deviation (S.D.).

**Figure 6.** Observed (red square) and model-predicted (red solid line) total plasma concentration-time profiles, and observed (black circle) and model-predicted (black dashed line) total brain concentration-time profiles in (A) FVB wild-type and (B) *Mdr1a/b*( $-/-$ )*Bcrp1*( $-/-$ ) mice ( $N = 3-4$  at each time point) following a single intravenous bolus (3 mg/kg). The observed data are presented as mean  $\pm$  standard deviation (S.D.).

**Figure 7.** Observed (red square) and model-predicted (red solid line) total plasma concentration-time profiles, and observed (black circle) and model-predicted (black dashed line) total brain concentration-time profiles in (A) FVB wild-type, (B) *Bcrp1*( $-/-$ ), (C) *Mdr1a/b*( $-/-$ ), and (D) *Mdr1a/b*( $-/-$ )*Bcrp1*( $-/-$ ) mice ( $N = 4$  at each time point) following a single oral dose (30 mg/kg). The observed data are presented as mean  $\pm$  standard deviation (S.D.). The observed data for the wild-type were previously reported (Laramy et al., 2017) and included in this present study, in order to compare with the three other genotypes that lack efflux transporter(s).

## TABLES

**Table 1.** Pharmacokinetic/metric parameters estimated from non-compartmental analysis (NCA) of total brain and plasma concentration-time profiles after administration of a single intravenous bolus of ponatinib (3 mg/kg) in FVB wild-type and *Mdr1a/b*( $-/-$ )*Bcrp1*( $-/-$ ) mice ( $N = 3-4$  at each time point). Data are presented as mean or mean  $\pm$  standard error of the mean (S.E.M).

Metric/Parameters	Plasma		Brain	
	FVB wild-type	<i>Mdr1a/b</i> ( $-/-$ ) <i>Bcrp1</i> ( $-/-$ )	FVB wild-type	<i>Mdr1a/b</i> ( $-/-$ ) <i>Bcrp1</i> ( $-/-$ )
$C_{\max}$ ( $\mu\text{g/mL}$ ) (Mean $\pm$ S.E.M.)	1.2 $\pm$ 0.05	1.1 $\pm$ 0.08	1.8 $\pm$ 0.1	4.7 $\pm$ 0.2
$T_{\max}$ (hr)	0.25	0.25	0.25	2
CL (mL/min/kg)	12.3	11.1	–	–
$V_d$ (L/kg)	3.2	3.4	–	–
Half-life (hr)	3.0	3.5	3.3	3.6
$AUC_{(0 \rightarrow t)}$ ( $\mu\text{g/mL} \cdot \text{hr}$ ) (Mean $\pm$ S.E.M.)	4.0 $\pm$ 0.3	3.96 $\pm$ 0.1	4.27 $\pm$ 0.2	42.1 $\pm$ 1.2
$AUC_{(0 \rightarrow \infty)}$ ( $\mu\text{g/mL} \cdot \text{hr}$ )	4.1	4.5	4.1	44.8
AUC based $K_p^a$	–	–	1.0	10.0
AUC based $K_{p,uu}^b$	–	–	0.11	1.1
Transient steady-state $K_p^c$	–	–	1.7	11.6
Transient steady-state $K_{p,uu}^d$	–	–	0.11	1.3
AUC based $DA^e$	–	–	–	9.9
Transient steady-state $DA^f$	–	–	–	6.9

<sup>a</sup> Calculated by  $[AUC_{(0 \rightarrow \infty), \text{brain}}]/[AUC_{(0 \rightarrow \infty), \text{plasma}}]$

<sup>b</sup> Calculated by  $[AUC_{(0 \rightarrow \infty), \text{brain}}]/[AUC_{(0 \rightarrow \infty), \text{plasma}}] \cdot [f_{u, \text{brain}}/f_{u, \text{plasma}}]$

<sup>c</sup> Calculated by  $C_{\max, \text{brain}}/C_{\text{p, tss}}$  Corresponding plasma concentration at that time ( $C_{\text{p, tss}}$ )

<sup>d</sup> Calculated by  $(C_{\max, \text{brain}} / \text{Corresponding plasma concentration at that time } (C_{p, \text{tss}})) * (f_{u, \text{brain}} / f_{u, \text{plasma}})$

<sup>e, f</sup> DA, distribution advantage due to the lack of efflux transporters, or  $K_{p, \text{knockout}} / K_{p, \text{wild-type}}$  or

$K_{p, \text{uu, knockout}} / K_{p, \text{uu, wild-type}}$

$V_d$ , volume of distribution

CL, clearance

**Table 2.** Pharmacokinetic/metric parameters determined by non-compartmental analysis (NCA) of total brain and plasma concentration-time profiles after a single oral dose (30 mg/kg) of ponatinib in FVB wild-type, *Bcrp1*( $-/-$ ), *Mdr1a/b*( $-/-$ ), and *Mdr1a/b*( $-/-$ )*Bcrp1*( $-/-$ ) mice ( $N = 4$  at each time point). Data are presented as mean or mean  $\pm$  standard error of the mean (S.E.M). Data for the wild-type were previously reported (Laramy et al., 2017) and included in this present study in order to compare with the three other genotypes that lack efflux transporter(s).

Metric/Parameters	Plasma				Brain			
	FVB wild-type	<i>Bcrp1</i> ( $-/-$ )	<i>Mdr1a/b</i> ( $-/-$ )	<i>Mdr1a/b</i> ( $-/-$ ) ) <i>Bcrp1</i> ( $-/-$ )	FVB wild-type	<i>Bcrp1</i> ( $-/-$ )	<i>Mdr1a/b</i> ( $-/-$ )	<i>Mdr1a/b</i> ( $-/-$ ) ) <i>Bcrp1</i> ( $-/-$ )
$C_{max}$ ( $\mu\text{g/mL}$ ) (Mean $\pm$ S.E.M.)	1.1 $\pm$ 0.1	0.98 $\pm$ 0.2	1.5 $\pm$ 0.4	1.0 $\pm$ 0.04	0.96 $\pm$ 0.07	1.0 $\pm$ 0.09	5.1 $\pm$ 0.7	13.1 $\pm$ 0.8
$T_{max}$ (hr)	2	4	2	4	2	8	4	4
CL/F ( $\text{mL/min/kg}$ )	46.6	48.2	39.1	43.3	—	—	—	—
$V_d/F$ ( $\text{L/kg}$ )	17.6	25.4	19.6	20.0	—	—	—	—
Half-life (hr)	4.4	6.1	5.8	5.3	5.7	6.6	4.3	5.5
$AUC_{(0 \rightarrow t)}$ ( $\mu\text{g/mL} \cdot \text{hr}$ ) (Mean $\pm$ S.E.M.)	10.4 $\pm$ 0.6	9.5 $\pm$ 0.8	12.1 $\pm$ 0.8	10.8 $\pm$ 0.6	8.3 $\pm$ 0.7	12.5 $\pm$ 0.7	45.0 $\pm$ 3.1	151.1 $\pm$ 7.4
$AUC_{(0 \rightarrow \infty)}$ ( $\mu\text{g/mL} \cdot \text{hr}$ )	10.7	10.4	12.8	11.5	8.8	13.7	46.4	163.6
AUC based $K_p^a$	—	—	—	—	0.82	1.3	3.6	14.2
AUC based $K_{p,uu}^b$	—	—	—	—	0.11	0.14	0.40	1.6
Transient steady-state $K_p^c$	—	—	—	—	0.87	1.6	4.9	12.7
Transient steady-state $K_{p,uu}^d$	—	—	—	—	0.11	0.18	0.54	1.4
AUC based $DA^e$	—	—	—	—	—	1.6	4.4	17.3
Transient steady-state $DA^f$	—	—	—	—	—	1.9	5.7	14.6

<sup>a</sup> Calculated by  $[AUC_{(0 \rightarrow \infty), \text{brain}}]/[AUC_{(0 \rightarrow \infty), \text{plasma}}]$

<sup>b</sup> Calculated by  $[AUC_{(0 \rightarrow \infty), \text{brain}}]/[AUC_{(0 \rightarrow \infty), \text{plasma}}] \cdot [f_{u, \text{brain}}/f_{u, \text{plasma}}]$

<sup>c</sup> Calculated by  $C_{max, \text{brain}} / \text{Corresponding plasma concentration at that time } (C_{p, \text{tss}})$

<sup>d</sup> Calculated by  $(C_{\text{max,brain}} / \text{Corresponding plasma concentration at that time } (C_{\text{p,tss}})) * (f_{\text{u,brain}} / f_{\text{u,plasma}})$

<sup>e,f</sup> DA, distribution advantage due to lack of transporters, or  $K_{\text{p,knockout}} / K_{\text{p,wild-type}}$  or

$K_{\text{p,uu,knockout}} / K_{\text{p,uu,wild-type}}$

CL/F, apparent clearance

$V_d/F$ , apparent volume of distribution

**Table 3.** Steady-state plasma and brain concentration, brain-to-plasma ratio, and distribution advantage of ponatinib after continuous intraperitoneal infusion (40 µg/hr) for 48 hours in FVB wild-type, *Bcrp1*(-/-), *Mdr1a/b*(-/-), and *Mdr1a/b*(-/-)*Bcrp1*(-/-) mice (*N* = 4 in each genotype). Data are presented as mean ± standard deviation (S.D.).

	Steady-state total concentration (µg/ml)		Total brain-to-plasma ratio (Kp)	Free brain-to-plasma ratio (Kp,uu) <sup>a</sup>	Distribution advantage (DA) <sup>b</sup>
	Plasma	Brain			
<b>FVB wild-type</b>	0.72 ± 0.66	0.53 ± 0.37	1.0 ± 0.51	0.11 ± 0.056	—
<b><i>Bcrp1</i>(-/-)</b>	0.42 ± 0.21	0.71 ± 0.30	1.8 ± 0.26	0.20 ± 0.029	1.7
<b><i>Mdr1a/b</i>(-/-)</b>	0.39 ± 0.14	1.3 ± 0.70	3.8 ± 2.5	0.42 ± 0.28	3.7
<b><i>Mdr1a/b</i>(-/-)<i>Bcrp1</i>(-/-)</b>	0.40 ± 0.34	6.1 ± 5.0*	15.6 ± 2.6*	1.7 ± 0.29*	15.0

\* Statistical difference (\* *P* < 0.05) compared to the FVB wild-type

<sup>a</sup> Calculated by  $Kp \cdot [f_{u,brain}/f_{u,plasma}]$

<sup>b</sup> DA, distribution advantage due to lack of transporters, or  $Kp_{knockout}/Kp_{wild-type}$  or  $Kp_{uu,knockout}/Kp_{uu,wild-type}$

**Table 4.** Data summary: Comparison of the total brain-to-plasma (Kp) estimates between different routes of administration, including a single intravenous bolus (3 mg/kg IV; *N* = 3-4 at each time point), oral dose (30 mg/kg PO; *N* = 4 at each time point), or continuous steady-state intraperitoneal infusion (40 µg/hr IP; *N* = 4 in each genotype). Data are presented as mean. Data for the wild-type after administration of a single oral dose were previously reported (Laramy et al., 2017) and included in this present study, in order to compare with the three other genotypes that lack efflux transporter(s).

Genotype	Total brain-to-plasma ratio (Kp)					Distribution advantage (DA)				
	<b>Method (A):</b> $Kp = [AUC_{(0 \rightarrow \infty), \text{brain}}] / [AUC_{(0 \rightarrow \infty), \text{plasma}}]$ <b>Method (B):</b> $Kp = \text{Transient steady-state concentration ratio} = C_{\text{max, brain}} / \text{Corresponding plasma concentration at that time point } (C_{\text{p, tss}})$ <b>Method (C):</b> $Kp = \text{Steady-state brain-to-plasma concentration ratio}$					Kp, knockout/Kp, wild-type				
	IV		PO		IP	IV		PO		IP
	A	B	A	B	C	A	B	A	B	C
<b>FVB wild-type</b>	1.0	1.7	0.82	0.87	1.0	-	-	-	-	-
<b><i>Bcrp1</i>(-/-)</b>	-		1.3	1.6	1.8	-	-	1.6	1.9	1.7
<b><i>Mdr1a/b</i>(-/-)</b>	-		3.6	4.9	3.8	-	-	4.4	5.7	3.7
<b><i>Mdr1a/b</i>(-/-) <i>Bcrp1</i>(-/-)</b>	10.0	11.6	14.2	12.7	15.6	9.9	6.9	17.3	14.6	15.0

**Table 5.** Pharmacokinetic parameters obtained from an open two-compartment model that described the total plasma concentration-time profiles from naïve pooled analysis of all genotypes ( $N = 4$  at each time point) after a single intravenous bolus (3 mg/kg) or oral dose (30 mg/kg). The parameters are presented as the mean estimate.

<b>Estimated Parameters</b>	<b>Mean</b>	<b>CV (%)</b>	<b>95% Confidence Interval (CI)</b>
$V_{\text{central}}$ (mL/kg)	1478.3	8.1	(964.8, 1991.9)
$K_{10}$ ( $\text{hr}^{-1}$ )	0.47	6.4	(0.34, 0.60)
$K_{21}$ ( $\text{hr}^{-1}$ )	2.34	19.2	(0.41, 4.3)
$K_{12}$ ( $\text{hr}^{-1}$ )	2.15	10.4	(1.2, 3.1)
$K_{\text{elim}}$ ( $\text{hr}^{-1}$ )	0.21	1.7	(0.20, 0.23)
$K_a$ ( $\text{hr}^{-1}$ )	0.28	11.5	(0.20, 0.36)
<b>Calculated Parameters</b>	<b>Mean</b>	<b>CV (%)</b>	<b>95% Confidence Interval (CI)</b>
$V_{u,\text{central}}$ (L/kg)	645.8	-	-
$\text{CL}_{\text{systemic}}$ (mL/min/kg) <sup>a</sup>	5.2	1.7	(4.8, 5.6)
Half-life (hr) <sup>b</sup>	3.3	1.7	(3.0, 3.5)

$V_{\text{central}}$ , volume of distribution of total drug in the central compartment

$V_{u,\text{central}}$ , volume of distribution of unbound (free) drug in the central compartment

$K_{10}$ , elimination rate constant from the central compartment

$K_{12}$  and  $K_{21}$ , intercompartmental transfer rate constants

$K_{\text{elim}}$ , terminal rate constant (elimination from the body) from Equation 4

$K_a$ , absorption rate constant after oral dosing

<sup>a</sup>  $\text{CL}_{\text{systemic}}$ , clearance of ponatinib (total drug) from the systemic circulation (body)

<sup>b</sup> Half-life of ponatinib (total drug) from the systemic circulation (body)

**Table 6.** Pharmacokinetic parameters obtained from the compartmental BBB model describing the brain and plasma concentration-time after administration of a single intravenous bolus (3 mg/kg IV; *N* = 3-4 at each time point) or oral dose (30 mg/kg PO; *N* = 4 at each time point) in FVB wild-type, *Bcrp1*(*-/-*), *Mdr1a/b*(*-/-*), and/or *Mdr1a/b*(*-/-*)*Bcrp1*(*-/-*) mice. Fixed values are left as blank (-). The parameters are presented as the mean estimate.

Route of Administration	Genotype	Parameters													
		$k_{in}$ (hr <sup>-1</sup> )		$k_{out}$ (hr <sup>-1</sup> )		$MTT_{brain}^a$ (hr)	$CL_{in}$ (mL/hr/kg)		$CL_{out}$ (mL/hr/kg)		$CL_{u,in}$ (mL/hr/kg)		$CL_{u,out}$ (mL/hr/kg)		
		Mean	CV (%)	Mean	CV (%)	Mean	Mean	CV (%)	Mean	CV (%)	Mean	CV (%)	Mean	CV (%)	
IV	WT	4.0*10 <sup>-5</sup>	-	7.7	10.2	0.13	0.059	-	0.066	36.6	25.8	-	225.8	22.5	
	TKO	4.0*10 <sup>-5</sup>	11.2	0.64	14.0	1.6	0.059	13.8	0.0055	37.9	25.8	11.2	18.7	24.4	
PO	WT	5.5*10 <sup>-5</sup>	-	12.4	2.7	0.081	0.081	-	0.11	35.3	35.2	-	361.6	20.2	
	Bcrp-KO	5.5*10 <sup>-5</sup>	-	8.2	18.2	0.12	0.081	-	0.070	39.6	35.2	-	239.4	27.0	
	Pgp-KO	5.5*10 <sup>-5</sup>	-	2.9	26.0	0.34	0.081	-	0.025	43.8	35.2	-	85.1	32.8	
	TKO	5.5*10 <sup>-5</sup>	16.2	0.65	15.7	1.5	0.081	18.1	0.0056	38.5	35.2	16.2	19.0	25.5	

<sup>a</sup> MTT<sub>brain</sub>, mean transit time in the brain; calculated by 1/ $k_{out}$

$k_{in}$ , tissue transfer rate constant into the brain

$k_{out}$ , tissue transfer rate constant out of the brain

CL<sub>in</sub>, total drug clearance into the brain

CL<sub>out</sub>, total drug clearance out of the brain

CL<sub>u,in</sub>, Free (unbound) drug clearance into the brain

CL<sub>u,out</sub>, Free (unbound) drug clearance out of the brain

WT, wild-type

Bcrp-KO, *Bcrp1*(-/-)

Pgp-KO, *Mdr1a/b*(-/-)

TKO, *Mdr1a/b*(-/-)*Bcrp1*(-/-)

**Table 7.** Total and free brain-to-plasma ratio (Kp,pred and Kp,uu,pred) and distribution advantage (DA,pred), using the pharmacokinetic parameters obtained from the compartmental BBB model describing the brain and plasma concentration-time profiles after administration of a single intravenous bolus (3 mg/kg IV; *N* = 3-4 at each time point) or oral dose (30 mg/kg PO; *N* = 4 at each time point) in FVB wild-type, *Bcrp1*(-/-), *Mdr1a/b*(-/-), and/or *Mdr1a/b*(-/-)*Bcrp1*(-/-) mice. The parameters are presented as the mean estimate.

Route of Administration	Genotype	Parameters										
		AUC <sub>(0→∞),predicted</sub> (Mean estimate)				Transient steady-state (Mean estimate)				Clearance based (Mean estimate)		
		AUC <sub>(0→∞), plasma</sub> (μg/mL*hr)	AUC <sub>(0→∞), brain</sub> (μg/mL*hr)	Kp,pred	DA,pred	C <sub>p,tss</sub> (μg/mL)	C <sub>max, brain</sub> (μg/mL)	Kp,pred	DA,pred	Kp,pred	Kp,uu,pred	DA,pred
IV	WT	4.0	3.6	0.89	-	1.2	1.1	0.89	-	0.89	0.11	-
	TKO	4.0	43.1	10.7	12	0.5	5.3	10.8	12.0	10.7	1.4	12.1
PO	WT	10.9	8.2	0.76	-	1.2	0.95	0.76	-	0.76	0.097	-
	Bcrp-KO	10.6	12.2	1.1	1.5	1.1	1.2	1.1	1.5	1.1	0.15	1.5
	Pgp-KO	11.2	35.9	3.2	4.2	1.1	3.4	3.2	4.2	3.2	0.41	4.2
	TKO	10.7	152.3	14.3	18.8	1.0	12.9	13.4	17.7	14.4	1.9	19.1

$$Kp,pred, \text{ calculated by } \frac{AUC_{(0 \rightarrow \infty), \text{ total brain, predicted}}}{AUC_{(0 \rightarrow \infty), \text{ total plasma, predicted}}} \cong \frac{\text{Total } C_{\text{max, brain}}}{\text{Corresponding total plasma concentration at that time } (C_{p, \text{tss}})} \cong \frac{CL_{\text{in}}}{CL_{\text{out}}}$$

Kp,uu,pred, free (unbound) derivative of brain-to-plasma ratio, calculated by

$$\frac{AUC_{(0 \rightarrow \infty), \text{ free brain, predicted}}}{AUC_{(0 \rightarrow \infty), \text{ free plasma, predicted}}} \cong \frac{\text{Free } C_{\text{max, brain}}}{\text{Corresponding free plasma concentration at that time } (C_{p, \text{tss}})} \cong \frac{CL_{u, \text{in}}}{CL_{u, \text{out}}}$$

DA,pred, distribution advantage (DA) due to lacking transporters; calculated by

Kp,pred, knockout/Kp,pred, wild-type, or Kp,uu,pred, knockout/Kp,uu,pred, wild-type

WT, wild-type

Bcrp-KO, *Bcrp1*(-/-)

Pgp-KO, *Mdr1a/b*(-/-)

TKO, *Mdr1a/b*(-/-)*Bcrp1*(-/-)

## FIGURES

Figure 1

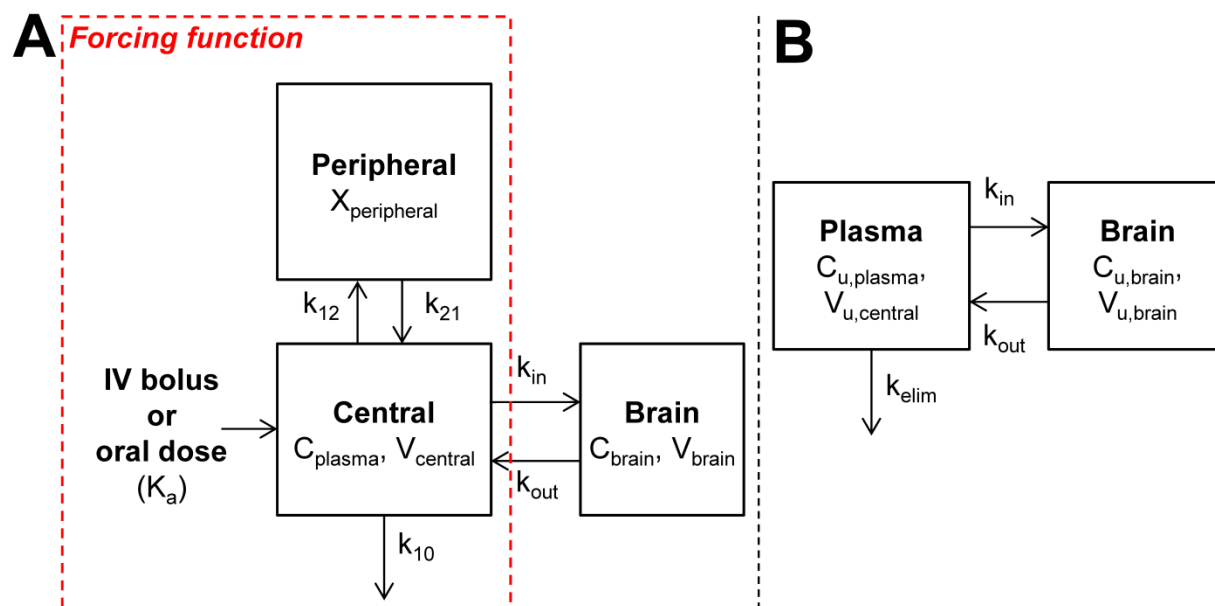


Figure 2.

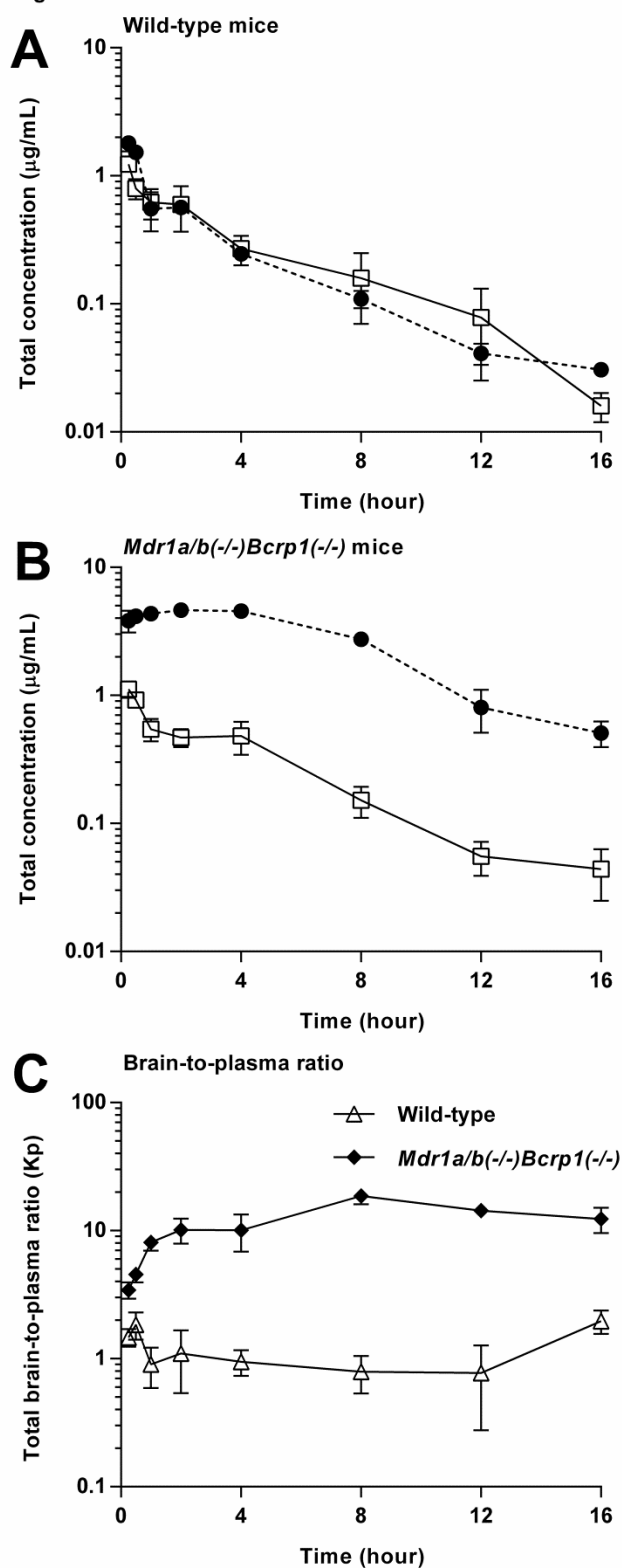


Figure 3.

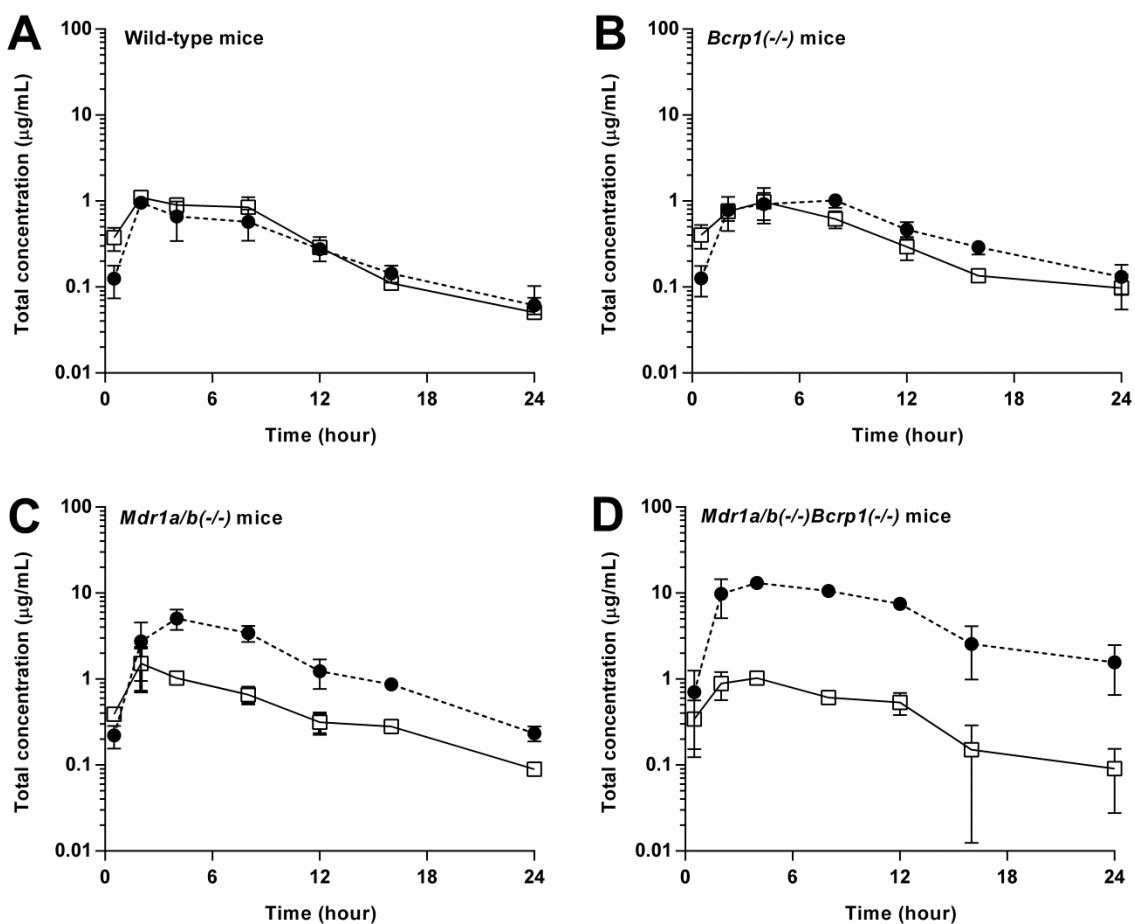


Figure 4.

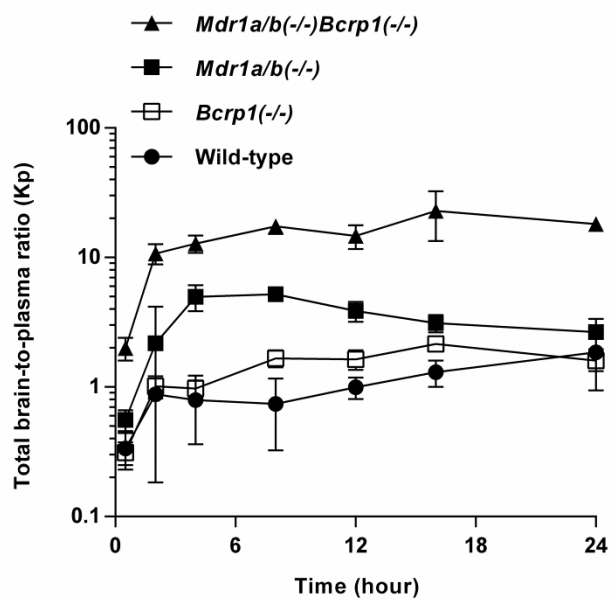


Figure 5.

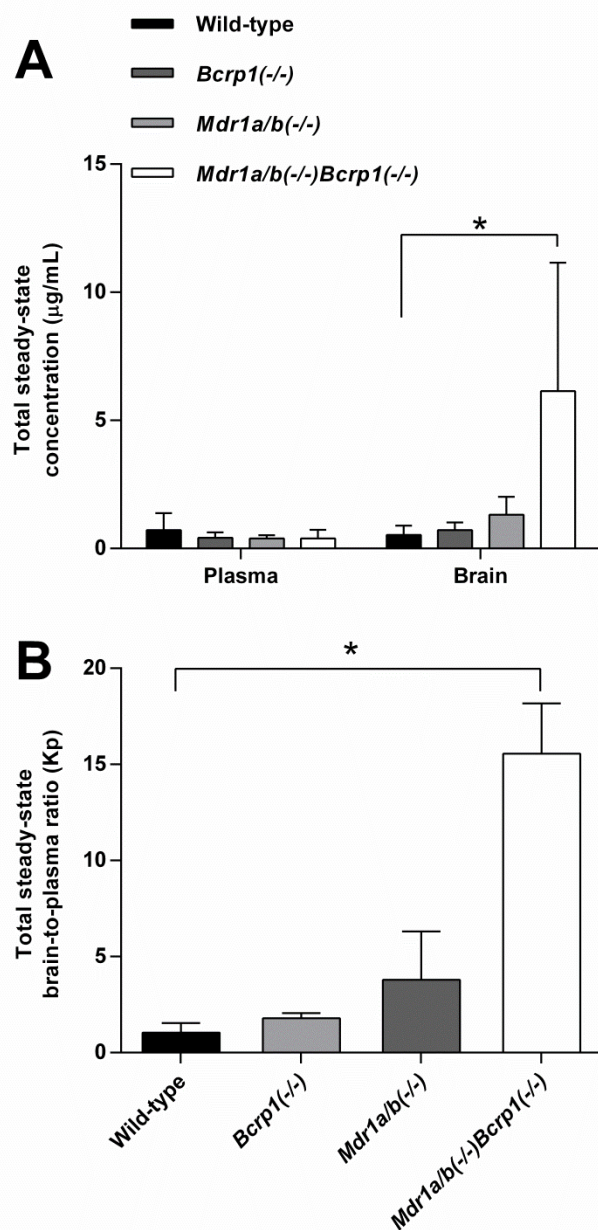


Figure 6.

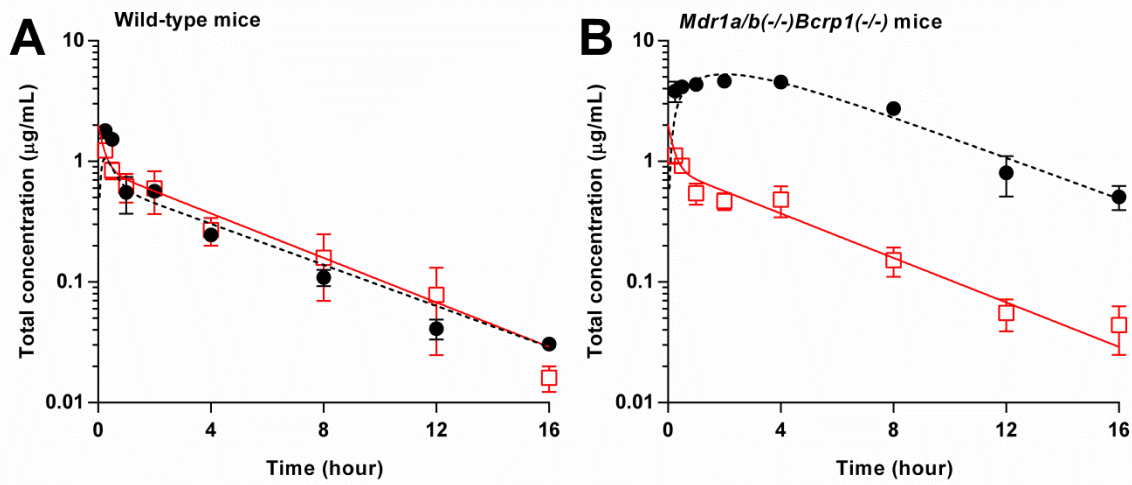


Figure 7.

